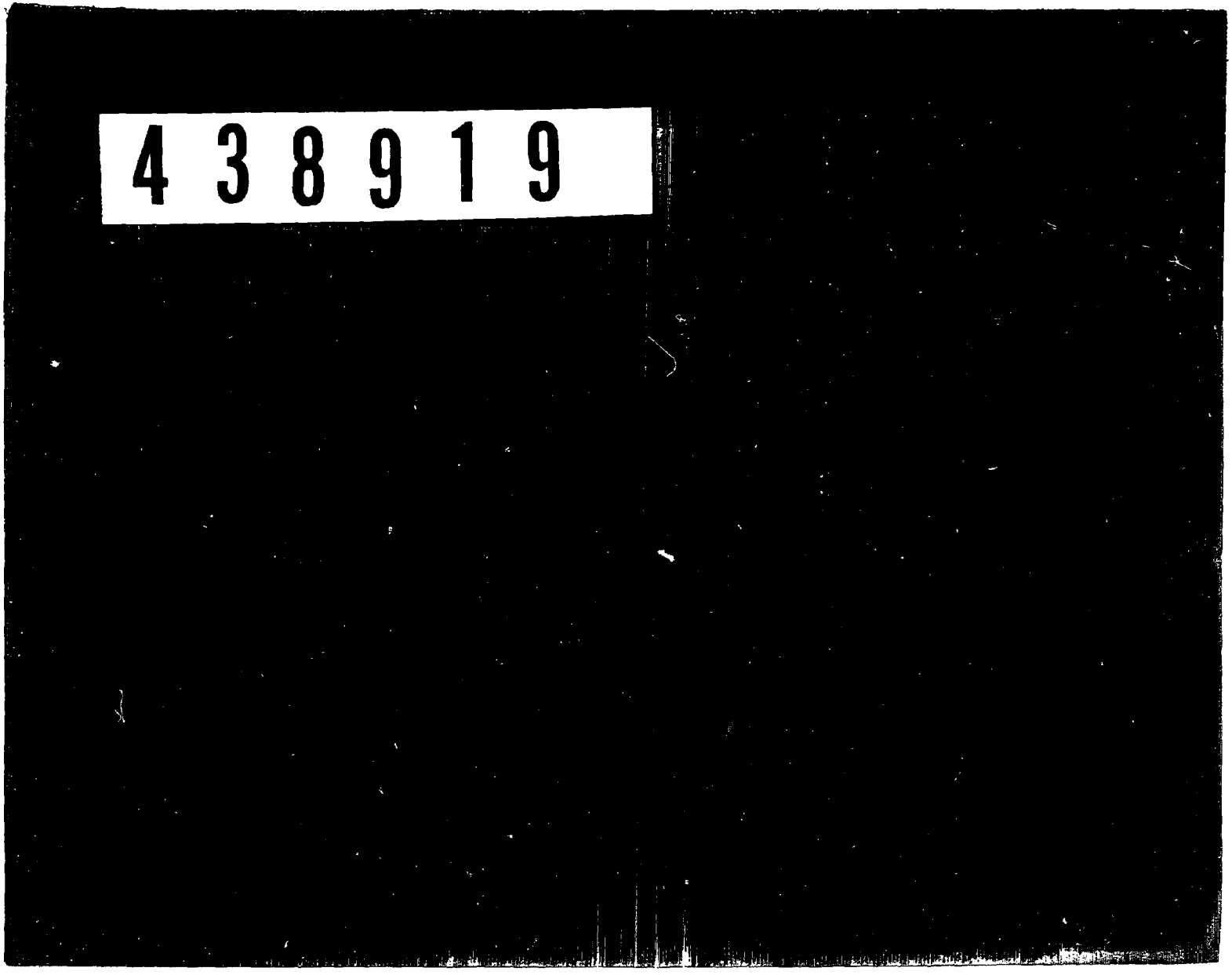
438919

ABSTRACT

MIONE, ANTHONY JOHN. Dispersed Uranium Monocarbide-Uranium Nuclear Fuel Material. (Under the direction of Robert Franklin Stoops).

The factors affecting the production of a nuclear fuel material consisting of a fine, uniform dispersion of uranium monocarbide in a uranium metal matrix were determined. Theoretical considerations indicated that a uniform dispersion of small, hard particles in uranium fuels would eliminate the "swelling" associated with release of fission gas products during irradiation that severely limits the usefulness of uranium fuel elements. Uranium monocarbide was selected for the dispersed phase because of its excellent combination of physical and nuclear properties.

Initially, techniques were developed which largely eliminated oxidation of the pyrophoric powdered raw materials during processing. Specimens were then prepared both by the cold-pressing, vacuum-sintering and by vacuum hot-pressing techniques at temperatures between 980°C and 1500°C. It was found that 10 to 15 per cent of finely dispersed uranium dioxide was necessary to prevent excessive growth of the uranium monocarbide particles. Under certain processing conditions the surfaces of the individual particles of uranium metal became coated with a layer of oxide. During hot pressing, applied pressures of 3500 to 4000 psi caused the oxide films to rupture, and this permitted the molten metal to infiltrate between the uranium monocarbide grains. In this process the uranium dioxide became uniformly distributed in the specimens. Cold pressing and

sintering did not produce dense specimens because the oxide films were not broken; and, when the particle of metal melted, the liquid metal remained encased in oxide. This effectively prevented liquid-phase sintering, and the temperatures were not high enough for densification by solid-state sintering.

Even when oxide was present during hot pressing, time and temperature were of primary importance in controlling densification and uranium monocarbide particle growth. Specimens with the desired microstructure were produced only by hot pressing at temperatures between 1132°C (the melting point of uranium) and 1150°C for three minutes or less. Higher temperatures or longer times resulted in excessive uranium monocarbide particle growth, while satisfactory densification was not obtained at lower temperatures.

The material developed in this investigation should be an outstanding nuclear fuel, consisting of a uranium matrix with a dispersion of approximately 10^{10} uranium monocarbide and to a lesser extent, uranium dioxide particles per cubic centimeter. This concentration should provide sufficient nucleation sites for fission product gases to make them collect in small bubbles. This would eliminate "swelling" which would be a significant advantage of this material when compared to uranium as a nuclear fuel material. Furthermore, the physical and nuclear properties of the uranium-uranium monocarbide-uranium dioxide material should make it desirable for use as a nuclear fuel. Irradiation testing of this material is planned.

(5) 643 400 North Carolina State Coll., Raleigh.

(6) DISPERSED URANIUM MONOCARBIDE - URANIUM NUCLEAR FUEL MATERIAL,

(10) by

ANTHONY J. MIONE,

A thesis submitted to the Graduate Faculty of
North Carolina State of the
University of North Carolina at Raleigh,
in partial fulfillment of the
requirements for the Degree of
Doctor of Philosophy

DEPARTMENT OF NUCLEAR ENGINEERING

RALEIGH

1963

APPROVED BY:

Chairman of Advisory Committee

BIOGRAPHY

Anthony John Mione was born in Brooklyn, New York, on March 8, 1927. Graduation from the United States Military Academy, West Point, New York, in 1949 was followed by a commission and flight training in the United States Air Force. He received his Master of Science degree in Nuclear Engineering from North Carolina State College, Raleigh, North Carolina, in 1953.

The succeeding five years were spent in various engineering, administrative, and management assignments in the Materials Laboratory, Wright-Patterson Air Force Base, Ohio. In 1958 he was transferred to Headquarters, Air Research and Development Command, Andrews Air Force Base, Maryland, where he served as a project administrator in the Nuclear Programs Office.

In 1960 he attended the Air Force Command and Staff College, Maxwell Air Force Base, Montgomery, Alabama. Graduate studies in Nuclear Engineering were resumed at North Carolina State College in 1961. Major Mione is a member of Sigma Xi, Tau Beta Pi, and Sigma Pi Sigma.

ACKNOWLEDGMENTS

The author appreciates the time and assistance given by the Advisory Committee: Dr. K. O. Beatty, Dr. H. A. Lamonds, Dr. J. Levine, Dr. R. F. Stoops, and Dr. N. Underwood.

Dr. R. F. Stoops, as the research advisor and chairman of the Advisory Committee, deserves particular mention. Without his encouragement, guidance, assistance, and technical and moral support, this investigation could not have been accomplished.

The author extends his appreciation to:

Dr. J. V. Hamme, who shared much of his equipment and experience in the laboratory;

Mr. Wade Griffin and his staff, who provided their skillful support in the fabrication and construction of most of the furnace and hot press equipment;

the staff of the Department of Engineering Research and its Director, Prof. N. W. Conner, who provided the necessary space, equipment, facilities, and administration support throughout the investigation; and,

the United States Air Force, through whose Institute of Technology attendance at the university was made possible.

The author's deepest appreciation is extended to his wife and family, without whose encouragement, support, and sacrifice this investigation would have been impossible.

The research was sponsored by the Joint USAEC-Euratom Research and Development Program under Contract Number AT-(40-1) - 2981. Their support and interest is gratefully acknowledged.

TABLE OF CONTENTS

	Page
LIST OF TABLES	v
LIST OF FIGURES	vi
INTRODUCTION	1
REVIEW OF LITERATURE	8
Cold Pressing and Sintering	10
Hot Pressing	11
Radiation Effects	13
Comparative Properties of U, UC, and UO_2	15
EXPERIMENTAL PROCEDURE	22
Materials	23
Equipment	25
Techniques	36
Production of Uranium Hydride	36
Preparation of Batch Compositions	38
Cold Pressing and Vacuum Sintering	41
Hot Pressing	43
Density Measurements	47
X-ray Analysis	47
Metallographic Techniques	48
RESULTS AND DISCUSSION	50
Cold Pressing and Vacuum Sintering	50
Hot Pressing	53
Uranium Dioxide as Grain Growth Inhibitor	61
Role of Oxide in Cold Pressing and Vacuum Sintering	62
Role of Oxide in Hot Pressing	65
SUMMARY	68
CONCLUSIONS	70
LIST OF REFERENCES	71
APPENDIX A	75
APPENDIX B	79

LIST OF TABLES

Table		Page
1	Cold pressing and sintering UC	11
2	Radiation damage in UC	14
3	Properties of U, UO_2, and UC	17
4	Impurities other than oxygen and nitrogen in uranium monocarbide raw materials	23

LIST OF APPENDIX TABLES

1	Specimen firing data	75
2	X-ray compositional analyses	79

LIST OF FIGURES

Figure		Page
1	Uranium-carbon constitutional diagram	9
2	Transverse rupture and impact strength vs. average grain size (60 TiC - 40 Ni)	16
3	Thermal conductivities of U, UO_2, and UC	21
4	Partial cut-away diagram of the horizontal vacuum-sintering furnace	27
5	Cross-section of the vertical hot press	30
6	Partial cross-section of "Tee" vacuum hot press	32
7	Vacuum hot press and associated instrumentation	33
8	Typical horizontal furnace cooling curve	44
9	Hot press cooling rate curves	46
10	Microstructures of cold-pressed specimens as a function of sintering temperatures	52
11	Microstructure of Specimen 55	54
12	Microstructure of Specimen 65	54
13	Hot press firing temperatures and times vs. grain sizes (900 - 1500°C)	55
14	Microstructure of Specimen 93	58
15	Hot press firing temperatures and times vs. grain sizes (1100-1200°C) - (Expanded section of Figure 13)	59
16	Microstructure of Specimen 94, low oxide content (6%) . .	60
17	Microstructure of Specimen 98, high oxide content (10-15%)	60
18	Sintering of cold pressed specimens	63
19	Sintering of hot pressed specimens	66

INTRODUCTION

The objective of this research was to develop a nuclear reactor fuel material consisting of uranium monocarbide and uranium metal. The unique characteristic of the desired material was its microstructure; viz, a very finely divided dispersion of uranium monocarbide particles, about 10^{12} particles per cubic centimeter, in a uranium metal matrix. Such a material was expected to combine the more advantageous fuel characteristics of both uranium metal and uranium monocarbide; i. e., high uranium density, high thermal conductivity, good thermal and mechanical shock resistance, resistance to growth or swelling during irradiation, and high utilization temperature. The primary problems anticipated in accomplishing these objectives were preventing grain growth of the uranium monocarbide particles, avoiding the formation of large zones of uranium metal, and preventing the oxidation of the constituents during processing.

The development of nuclear power has been delayed by the lack of completely suitable materials. This is particularly true in the case of fissionable fuel materials. Since the fuel materials, to a large extent, dictate the technical and economic feasibility of advanced designs, the development of suitable fuel components that can meet the conditions demanded by designers is considered to be the most important requirement for the success of the nuclear power industry (27).

The availability of uranium, as compared to plutonium or thorium, has made it the most commonly used fissionable fuel material for nuclear reactors. The use of elemental metal, however, severely limits the power,

fuel lifetime, and, consequently, the economic feasibility of nuclear power reactors. Massive uranium metal experiences great physical instability due to creep, temperature- and irradiation-induced crystallographic transformations, and the expansion of gases resulting from fission. Fuel slug lengths may change as much as ten to twenty per cent at fission levels as low as a few tenths of one per cent of the available uranium atoms. In almost all reactors, the useful lifetime of the fuel elements will have been reached if serious dimensional changes occur in the fuel. Large variations in heat transfer coefficients, flux distributions, and fuel element temperatures can cause local failures. Highly distorted, or "stuck" fuel elements are very objectionable since they lead to protracted reactor shutdowns and a loss of utility (27).

In spite of these disadvantages, uranium metal has the highest possible fissionable atom density, the high thermal conductivity and thermal shock resistance typical of metals, and the high mechanical shock resistance desired in reactor fuel elements. Uranium-metal alloys developed to retain these characteristics while minimizing the disadvantageous characteristics of the metallic fuels require the addition of non-fissioning, non-moderating, and neutron-absorbing atoms to the fuel material. Such alloying additions contribute nothing to the fission process, but rather lower the density of fissionable atoms and act as neutron poisons. The uranium alloys, however, do permit reactor operation for extended periods of time without fuel failure.

Another approach, the use of refractory compounds of uranium, principally uranium dioxide (UO_2), allows high temperature operation, but

the disadvantages enumerated above must be extended to include the characteristics typical of ceramic materials. In spite of poor thermal and mechanical shock resistance, low thermal conductivity, low uranium atom density, and low bulk density, the stability of uranium dioxide at high temperature and irradiation levels has brought it into widespread use.

As reactor designs improve, the demand grows for better nuclear fuels capable of operating at higher temperatures for longer times. Oxide fuels, because of their low thermal conductivity, limit the reactor power levels unless the fuel cores are allowed to melt. Significant problems with differential thermal expansion and fission gas release are encountered under such conditions (2, 29).

A fuel material which appears to combine the advantages of both metallic and ceramic fuels is uranium monocarbide (UC). The melting point of UC is nine-tenths of that of UO_2, while its thermal conductivity is about eight to ten times that of UO_2 and two-thirds that of uranium metal. The density of UC is about half way between UO_2 and uranium, while its fissionable atom density is thirty per cent higher than that of UO_2 (3,48). Irradiation tests up to 14,000 megawatt days per ton (MWd/t) fuel utilization at temperatures up to 800°C showed the dimensional stability and fission product retention ability of UC to be comparable to UO_2 operating at only 400°C (48). Every material has its disadvantages, however, and UC is no exception. The pure carbide has the typically poor mechanical properties of ceramics, it oxidizes readily at room temperature, and it is highly pyrophoric when in sufficiently small particle size.

To take advantage of the desirable properties of both uranium monocarbide and uranium metal, fuel elements containing both materials have been proposed (36, 55). The unique aspect of this research is the emphasis on grain size control of uranium monocarbide dispersed in a uranium metal matrix. Such a material is expected to suffer minimal physical distortion caused by internal gas pressure build up during irradiation. Internal stress developed by fission gases can be extremely high. About 3×10^3 volumes of gas (Xenon and Krypton) are produced per unit volume of uranium that fissions (4). This gas is formed fairly uniformly throughout the bulk of the fuel material, preferentially nucleating as bubbles at discontinuities such as grain boundaries and dislocations (4, 5, 16). The growth of certain of these gas bubbles and the local overstressing of the fuel material results in macroscopic swelling of the fuel element. The referenced authors have postulated that massive swelling may be decreased by increasing the number and decreasing the size of the gas bubbles, since smaller bubbles would increase the chances for surface tension restraint on the gas. The internal bubble pressure is a direct function of the bubble radius, according to

$$P_i = P_{external} + \frac{2\sigma}{r}$$

where

σ = surface tension of the bubble-matrix interface

r = gas bubble radius

thus, a much higher gas pressure could be restrained in small bubbles than in large ones by some specified creep or tensile strength of the fuel

material. The overall volume of gas, therefore, that could be trapped and retained in a volume of fuel material without distortion would be very much higher with extremely small, evenly distributed gas bubbles.

Nucleation sites spaced about 0.3-0.5 micron apart (1 micron = 10^{-4} centimeters) have been found to be optimum (16). This spacing appears to provide the best balance between the largest possible number of bubble nucleation sites and the smallest separation between bubbles to minimize agglomeration of adjacent bubbles. A complex balance between diffusion lengths for the gases formed, temperature, and physical strength of the fuel material in the walls separating the bubbles really determines the optimum bubble spacing. A conservative objective selected for this research is the provision of bubble nucleation sites in the form of particle grain boundaries spaced approximately one-half micron apart. To obtain such a particle spacing, a particle density of from 10^{10} to 10^{12} per cubic centimeter is required. Such a particle density should provide sufficient grain boundary sites for homogeneous gas bubble nucleation to distribute the fission-gas-induced stresses.

The use of a uranium metal matrix for the finely dispersed uranium monocarbide particles offers a number of advantages. No degradation of the uranium atom density, as would occur with any other matrix material, results. The matrix material, as well as the dispersant, can contribute to fission efficiency. The use of uranium metal avoids the necessity of adding materials which absorb neutrons and further lower the neutron efficiency of the reactor. The availability of free uranium atoms will provide sinks for liberated carbon atoms (from the fissioned UC) which might

otherwise carbonize and embrittle cladding materials to the point of failure. The high thermal conductivity of uranium will prevent excessive fuel core temperatures even at the high fuel surface temperatures required for good thermal efficiency of the reactor system. The continuous uranium metal matrix will provide the necessary mechanical and thermal shock resistance to minimize fuel element manufacturing and handling problems. The ductility of the matrix metal will permit some internal stress relief and avoid brittle failure typical of ceramics.

The very fine dispersion of the ceramic phase should in turn improve the physical properties of the uranium matrix. The random orientation of very small grains of uranium between carbide particles should eliminate the preferred growth experienced with oriented uranium fuel materials. The UC phase should act as an excellent dispersion hardener for the uranium metal, since the strongest such structures are those in which the slip and recovery inhibitor phase is extremely small (less than two microns and preferably less than one micron) and is distributed uniformly throughout the matrix (14). Strengthening of the metallic matrix results from a number of phenomena. Slip failure within thin metal films between refractory carbide grains is minimized by the restraining forces exerted by the hard particles. The thin films also exhibit the increase in strength usually associated with films and whiskers when the particle spacings approach the micron range.

The intimate mixture of carbon with uranium fuel atoms can provide an additional nuclear advantage. The carbon atoms, which have good neutron-moderating properties, are able to rapidly decrease the fission

neutron energies to below the resonance absorption energies of uranium-238. The resultant increase in the resonance escape probability (p) of the fuel should more than compensate for the capture of neutrons by the carbon atoms in the high neutron flux field expected in the fuel.

The objective of this research, therefore, is to produce an improved nuclear reactor fuel which combines the advantages of both uranium metal and uranium monocarbide in a single material, while minimizing the disadvantages of both phases. The desired fuel material consists of finely divided uranium monocarbide particles dispersed uniformly in a uranium metal matrix, with a combined particle density of about 10^{12} particles per cubic centimeter. Powder metallurgical procedures and techniques are used to minimize grain growth and recrystallization of the very fine starting powders.

REVIEW OF LITERATURE

The search for pertinent literature was conducted through the files of the Armed Services Technical Information Agency, the Library of Congress, the United States Patent Office, the library of North Carolina State of the University of North Carolina at Raleigh, and of reports received from other USAEC-Euratom contractors.

Although uranium monocarbide has been recognized as a possible reactor fuel material for many years, intensive research began only about four or five years ago. The principal impetus for research was the potential for higher efficiencies in sodium-cooled reactors, where the high thermal conductivity of UC matched the high heat removal capacity of the liquid metal coolant better than did UO_2 (35). The excellent thermal, physical, and electronic properties of uranium monocarbide, also, made it an attractive material for use in other advanced reactor and thermoelectric conversion concepts (20, 34, 35, 38).

Figure 1 is a reproduction of the binary uranium-carbon constitution diagram reported by Rough and Chubb (42). Only UC, of the three reported carbides, appears suitable for reactor applications. UC_2 has been reported to be metastable at room temperature, to undergo a phase transformation at 1750 to 1765°C, and to be unstable in a radiation environment (1, 18). U_2C_3, on the other hand, can be formed only by special heat treatment or stress, and it decomposes to UC and UC_2 above 1780°C (33).

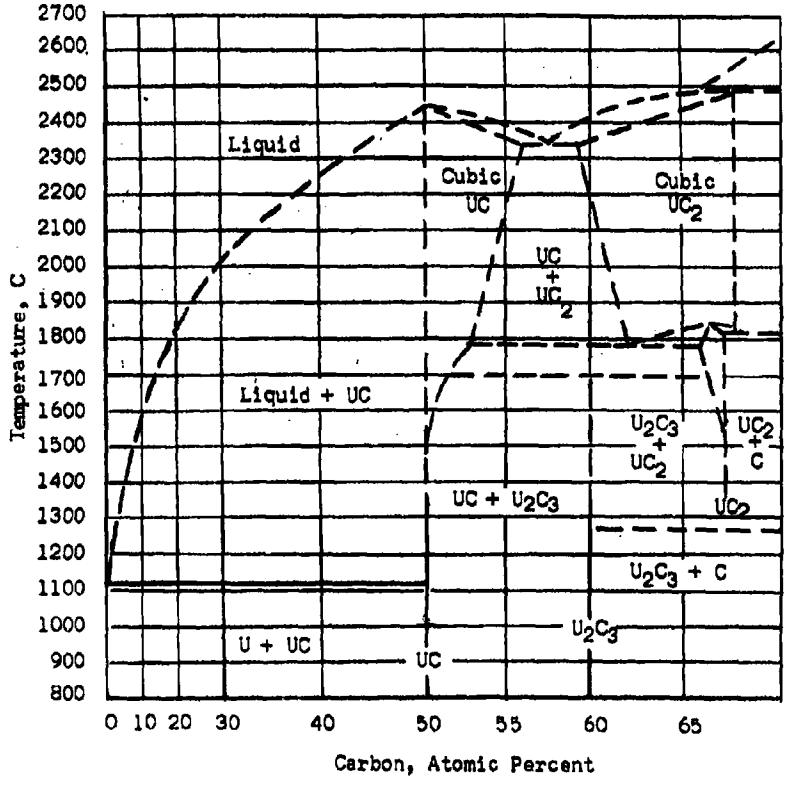

Figure 1. Uranium-carbon constitutional diagram

A great volume of information on the properties of metallic uranium is widely available (23, 26, 27, 28). Such properties as are of interest in this investigation are cited later in this section.

Cold Pressing and Sintering

A large number of investigators have reported their efforts to cold press and sinter uranium monocarbide. Table 1 reflects some of the results of these investigations.

Both Taylor and McMurtry (50) and Bolta and Strasser (7) reported that additions of uranium hydride or uranium metal up to 10 weight per cent did not greatly increase the density of the final product. It should be pointed out that both teams of investigators sintered in vacuum at temperatures considerably higher than the melting point of uranium. Watrous (53), on the other hand, reported obtaining bulk densities of 88-90 per cent of theoretical by compacting at 80,000 - 100,000 pounds per square inch and sintering for one hour at 1260-1370°C in helium. These specimens were formed from 50-70 volume per cent UC mixed with U powders.

Williams (55) patented his process for fabricating UC-U cermets from uranium and carbon powders at 1000-1100°C. He obtained hypostoichiometric, stoichiometric, and hyperstoichiometric compacts, but no control of grain size was reported.

Hot Pressing

In order to obtain higher bulk densities, many of the investigators attempted using hot-pressing techniques. Hot pressing offers significant

Table 1. Cold pressing and sintering UC

Investigator(s)	Temperature °C	Pressure psi	Time Hr.	Density gm/cm^3
Bolta and Strasser (7)[a]	1850	40,000	1	12.7-13.0
Finley, et al. (12)[b]	2050	--	1/2	12.6
Kalish (24)[c]	1800	70,000	3	12.3
Murray (32)[d]	2000	--	-	12.0
Rough and Chubb (39)	1900	80-100,000	-	12.3
Taylor and McMurtry (50)[e]	1940	16,500	-	12.1
Tripler, et al. (51)[f]	1800	--	3	12.4

[a]Small particle size, about one micron, was found to be of prime importance in achieving high densities.

[b]Fine powders (less than 10 microns average size) had to be used to obtain any appreciable densification.

[c]Large grains of UC with small amount of free uranium at the grain boundaries. The presence of free uranium appreciably raised the density.

[d]Large grain size in very brittle material.

[e]Fe additions (0.1-1.0%) improved the sinterability of UC, but re-crystallization and grain growth were accelerated (49).

[f]Grain size of 14.7 micron starting material was large and irregular.

advantages in the preparation of high-temperature, brittle materials such as UC. A number of techniques have been reported. Bolta and Strasser (7) and Murray (31) attempted to simultaneously synthesize and fabricate finished UC shapes by hot-pressing uranium metal powder and carbon. Bulk densities of 13.3 gm/cm^3 were obtained, but the material had a non-uniform distribution of phases.

Chubb and Rough (9), Finley, et al., (12), and Meyerson, et al., (30) obtained bulk densities from 90 to 99 per cent of theoretical by hot-pressing UC at 1320 to 2000°C. Meyerson, et al., in addition, obtained porosities of less than 5 per cent by hot-pressing a 31.8-weight-per cent, uranium-uranium carbide mixture for two hours at 1700°C.

Hot pressing offers distinct advantages when grain size control is desired. Very dense materials can be produced without long sintering times at temperatures where rapid grain growth occurs (46). Since grain growth is not a necessary condition for densification to take place, very fine particle sizes can be retained by hot pressing (31). The use of fine powders, however, led to the formation of variable amounts of UO_2 in some of the hot-pressed specimens produced by Rough and Chubb (41).

Although the presence of a reactive liquid phase during hot pressing can facilitate material transport (12), excessive amounts of uranium metal may be detrimental during reactor operation. Large lakes of free uranium may swell, melt, or react with the fuel cladding during high temperature operation (48). The major problem reported by most of the investigators was obtaining a homogeneous distribution of phases in UC-U materials produced by hot pressing.

Radiation Effects

The UC fuels appear particularly attractive because of the excellent radiation stability determined in preliminary tests. Table 2 summarizes the results of a number of in-pile experiments.

Rogers and Adam (38) reported that 85 percent of the irradiation damage to UC is annealed out at temperatures of about 640°C (1184°F), and that essentially all the damage is annealed out at about 700°C (1292°F). Confirmation of complete annealing at 700-730°C was reported by Griffiths (17).

One of the major requirements demanded of a fuel material is dimensional stability in conjunction with fission-product gas retention. The many theories (8, 17, 42, 54) which attempt to explain the formation and growth of gas bubbles agree that as the number of gas nucleation sites is increased, the probability of macroscopic failure of the fuel material is decreased. Barnes (5), Boltax (8), and Greenwood (15) have observed bubble formation along discontinuities, particularly at grain boundaries, in irradiated materials. Greenwood (15) proposed that gas bubble nucleation sites spaced approximately 0.5 micron apart would be best. Smaller spacings would approach the diffusion lengths of the fission product gases and lead to rapid coalescence of adjacent bubbles. Larger spacings would require each bubble site to contain the gas formed in a larger volume of surrounding material. Since the spherical volume surrounding the nucleation point varies with the cube of the radius, very large increases in gas volumes per bubble would be involved as the number of nucleation sites is decreased.

Table 2. Radiation damage in UC

Investigator	Fuel Burn-up mwd/t	Fuel Temperatures °F/°C
Hare, et al. (19)	10,800	800-1375/420-740
Hayward (21)	10,000	1600/870
NAA-SE-7400 (1)	725,000	1200/650
Rough et al. (44)	6,400	1830/1000

[a]Cracking evident in all specimens, primarily associated with thermal stress failures. Density decreases ranged from about 0.7 to 2.5 percent.

[b]No indication that limit of fuel has been reached. Damage primarily limited to cracking.

[c]Density decrease of 0.6 to 2.5 percent is small compared to that for uranium or uranium alloy fuels. Surface damage apparently due to oxygen absorption from NaK coolant used in the experiment.

Grain size control in powder metallurgy can be exercised by grinding the constituent powders to the desired size before fabrication, and preventing grain growth during sintering. Quatinez (37) obtained submicron powders of both ductile and brittle metals by using various grinding aids, among them stearic acid, during extended milling of the powders. The grinding aids coat the freshly formed, highly active surfaces and prevent rewelding of the particles once they are reduced in size. Grain growth in UC was reported (1) for nominally stoichiometric specimens heated for two hours at 1900°, 1700°, 1500°, and 1400°C. Grain growth was not observed, however, in specimens heated for the same time at 1300°C.

Binder and Steinitz (6) reported an additional advantage of a fine-grained microstructure. The increase in both impact strength and modulus of transverse rupture as a function of grain size is shown in Figure 2.

Comparative Properties of U, UC, and UO_2

The properties of uranium, uranium monocarbide, and uranium dioxide have been tabulated in Table 3, so that they may be easily compared. Figure 3 illustrates the differences in the thermal conductivities of the three materials.

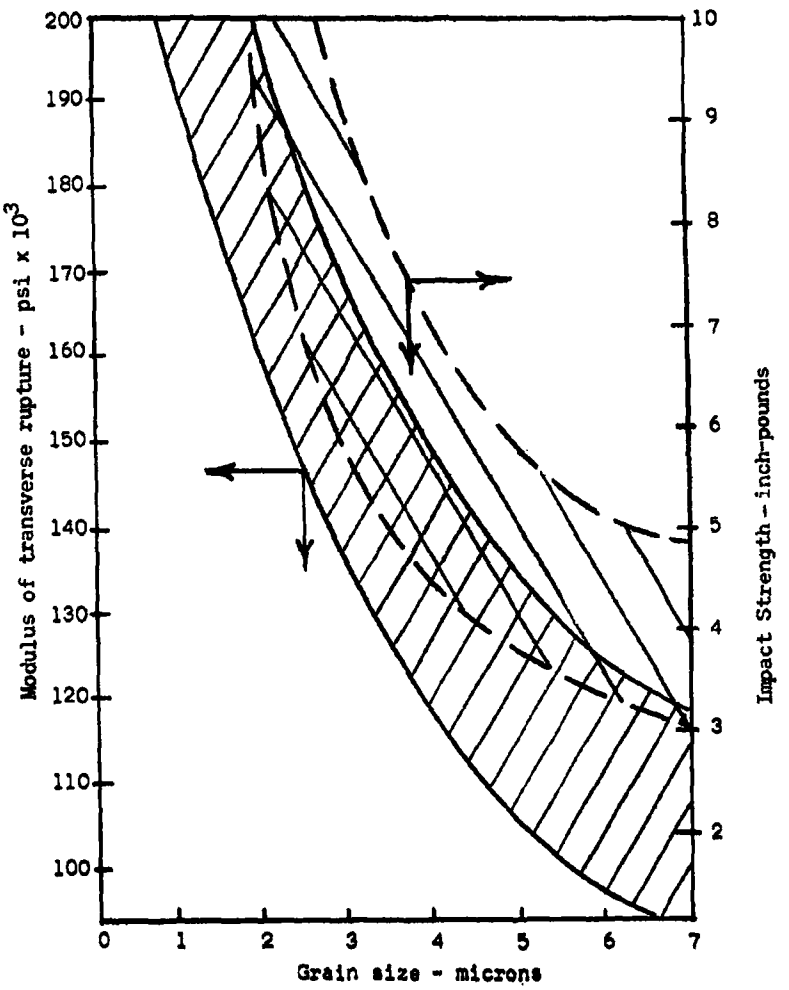

Figure 2. Transverse rupture and impact strength vs. average grain size (60 TiC - 40 Ni)

Table 3. Properties of U, UO_2, and UC

	Uranium	Uranium Dioxide	Uranium Monocarbide
Chemical symbol	U	UO_2	UC
Molecular weight	238.18	270.07	250.08
Density (gm/cm^3) (Theoretical at 25°C)	19.05	10.97	13.63
Uranium density (gm/cm^3) (43)	19.05	10.5	12.97
Melting point (°C) (43)	1132	2750	2350
Boiling point (°C) (43)	3818	4100	4370
Crystal structure (43)	α = orthorhombic (to 668°C) β = tetragonal (668-774°C) γ = cubic (774-1130°C)	cubic (fluorite)	cubic (NaCl)
Lattice Parameter (Å) at 25°C	a_o = 2.8541 (26) b_o = 5.8692 c_o = 4.9563	4.467 (18)	4.961 (18)
Bond (43)	metallic	covalent and ionic	covalent and metallic[a]

Continued

Table 3 (Continued)

	Uranium	Uranium Dioxide	Uranium Monocarbide
Thermal conductivity (cal/sec-cm-^{o}C)	0.065-0.104 (26)	0.018-0.008 (47) (100-700^{o}C)	0.06 (100-700^{o}C) (40)
Electrical resistivity (43) (megohm/cm)	29	10^{2}-10^{5} (b)	40-129 (0.02-9.3 w/o carbon)
Thermal coefficient of expansion ($cm/^{o}F)x10^{6}$ (43)	a directions - 19.5	5.1 (81-753 F)	5.6 (68-900^{o}F) (c)
	b directions - 4.72	6.0 (752-1472 F)	6.4 (68-1600^{o}F) (c)
	c directions - 8.1 (77-1157 F)	7.0 (1472-2300 F)	
Specific heat (C_p) (cal/gm mole ^{o}K)	α- 3.15+8.44x10^{3}K+0.8x10^{5}K^{-2}	0.071+6x10^{-6}K-1466K^{-2}	7.6+2.85x10^{-3}K
	β- 10.38 (26)	(0-1500^{o}K) (26)	(298-2400^{o}K) (33)
	γ- 9.10		
Vapor pressure (log P) (mm Hg)	$\frac{-23,300}{^{o}K}$ + 8.583 (27)	71x10^{-6}-72x10^{-3} (26) (1600-2000^{o}C)	$\frac{-F_v}{4.575}$ T
Free energy of formation - 25^{o}C cal/mole		-246,600 (26)	-41,000 (33)
Fission-Absorption cross-section ration	0.55 (11)	0.55 (11)	0.55 (11)

Continued

Table 3 (Continued)

	Uranium	Uranium Dioxide	Uranium Monocarbide
Hardness -25°C	290 VHN (d) (26)		Cast 560 VHN (33)
	218 DPH		Sintered 750-800 VHN
Tensile strength (ultimate psi)	67,000 (as cast) (23)		
	200,000 (β treated)		
Yield strength	26,000 (as cast)		10,000-14,000 (11) (transverse rupture)
	76,000 (β treated)		
Bond strength (psi)			50,000 (32)
Compressive strength (psi)	110,000 (10% set) (23)	150,000 (26)	51,000-66,000 (11)
Young's modulus ($x10^{-6}$ psi) (43)	25.5	25-30	32 (as cast)
Creep strength	0.22% elongation in 1,000 hrs. at 350°C and 8800 psi (26)		0.18% elongation at 810°C and 800 psi with 2% C (5)

Continued

Table 3 (Continued)

	Uranium	Uranium Dioxide	Uranium Monocarbide
Resistance to thermal cycling	Phase transformation at 644°C and 766°C cause growth and grain boundary cracking during thermal cycling (26)	3 cycles, 1000° to RT cracked (28)	500 cycles, 200-1000°C (3) no fracture 2000 cycles, 100-750°C no change (28) 20 cycles, 1000°C to RT no change[e] (28)

[a]UC bonding probably consists of 4 covalent and 2 metallic bonds per uranium atom accounting for partly metallic, partly nonmetallic behavior.

[b]UO_2 behaves like semiconductor, surface effect is important. Resistivity decreases with increasing temperature.

[c]UC measurements made on cast specimens, sintered powder specimens would probably be lower.

[d]Highly dependent on impurity or alloy additions.

[e]Thermal shock tests at thermal gradients of up to 800°C indicate that the resistance of arc cast UC is greatly superior to that of UO_2, and roughly comparable to that of some grades of alumina (45).

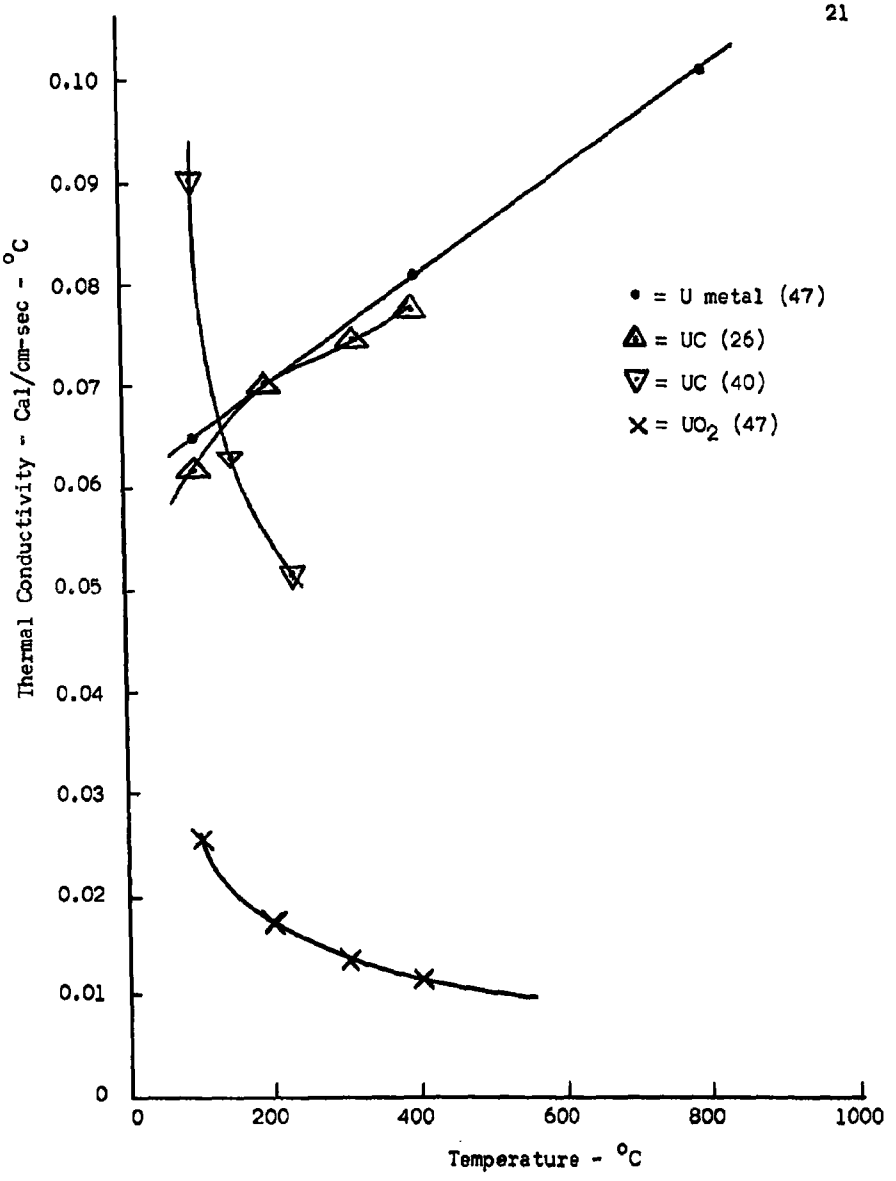

Figure 3. Thermal conductivities of U, UO_2, and UC

EXPERIMENTAL PROCEDURE

The experimental procedures used in this investigation will be briefly summarized here, and followed by a detailed description of the equipment and techniques used to obtain the reported results. The materials used in this investigation, principally uranium metal and uranium monocarbide, were obtained from commercial sources. In order to be able to reduce the ductile uranium metal to the desired small particles, the cleaned uranium metal chips were converted to uranium hydride, which is more amenable to grinding. Precalculated quantities of uranium hydride powder, uranium monocarbide powder, protective binders and milling assist agents were then loaded into grinding mills with reagent cyclohexane. The powders were reduced in average size to less than one micron by milling at least 70 hours. The powders so produced were dried in an argon-filled glove box and either pressed into pellets for subsequent vacuum sintering or loaded as powder into molybdenum-lined graphite dies for hot pressing. The specimens so prepared were fired at temperatures up to 1500°C and pressure up to 4000 psi and allowed to furnace cool prior to examination and analysis. X-ray diffraction analyses of the powders before firing and of the specimens after firing indicated the degree and/or changes in impurity concentrations, principally of uranium dioxide. Physical and bulk density measurements were made on all specimens which were not visibly unsatisfactory. Metallographic techniques were used to evaluate the structure of the specimens, and to obtain a statistical estimate of porosity and phase distribution in the fired specimens.

Materials

The raw materials used for this investigation consisted of:

1. Uranium monocarbide (UC). Minus 20 plus 140 mesh UC was purchased from the Nuclear Materials and Equipment Corporation, Apollo, Pennsylvania. An x-ray analysis of this product indicated 3 per cent UO_2, 2 per cent UC_2, and the remainder UC. Chemical analysis indicated 4.31 per cent combined carbon, 0.041 per cent free carbon, 0.30 per cent oxygen and 0.079 per cent nitrogen. The analysis of the material as supplied by the producer is given in Table 4.

Table 4. Impurities other than oxygen and nitrogen in uranium monocarbide raw materials

Element	Analysis (PPM)	Element	Analysis (PPM)
Fe	90	Pb	3
B	less than 0.5	Cr	less than 10
Co	less than 5	Si	300
Mn	less than 10	Ti	15
Al	less than 20	Ni	15
Mg	less than 10	Mb	10
Sn	less than 2	V	3
Cu	6		

The uranium carbide powder as received from the supplier was separated into three size fractions: 100 mesh, 40 mesh, and larger than 40 mesh. The two finest particle size ranges were used because of the difficulty experienced in reducing the large particles to sub-micron powder within reasonable milling times. The large grains were manually reduced to the finer sizes in a steel morter and pestle before use.

It was found that the carbide was slowly oxidized by reaction with traces of moisture in the argon-filled glove boxes. The larger carbide particles were separated from the fine oxide by screening, and only the cleaned carbide used in the mill batches. Although some oxide was introduced into the batches, it was minimized by this screening step.

2. Uranium (U). The uranium metal was purchased in the form of chips from the City Chemical Company, New York, New York. A chemical analysis of the material indicated 0.010 per cent oxygen, 0.002 per cent nitrogen, 0.008 per cent combined carbon, and less than 0.001 per cent free carbon.

3. Uranium hydride (UH_3). The UH_3 used in this investigation was made in the laboratory by reacting hydrogen with uranium chips. X-ray analyses of the hydride batches indicated a UO_2 content varying from a trace to about three per cent, with the remainder UH_3. A chemical analysis of the UH_3 indicated an oxygen content of 0.672 per cent, a hydrogen content of 1.22 per cent, and a nitrogen content of 0.018 per cent, with the remainder uranium.

4. Argon (A). Argon was obtained from the Southern Oxygen Company, Raleigh, North Carolina. A mass spectrographic analysis indicated 99.6 per cent A, 0.04 per cent N_2, and traces of O_2 and CO_2.

5. Hydrogen (H_2). The hydrogen, used for producing UH_3, was obtained from Southern Oxygen Company, Raleigh, North Carolina. A typical supplier's analysis of this gas indicated 99.8 per cent H_2, 0.2 per cent (O_2 + N_2), and less than 0.02 mg of water per liter.

6. Naphthalene ($C_{10}H_8$). The naphthalene, used as a binder and protective coating for the powder, was reagent grade obtained from the J. T. Baker Chemical Company, Phillipsburg, New Jersey.
7. Stearic Acid (CH_3-$(CH_2)_{16}CO_2H$). The stearic acid, used as a milling assist agent and die lubricant, was reagent grade obtained from Matheson, Coleman, and Bell, Division of the Matheson Company, Incorporated, East Rutherford, New Jersey.
8. Cyclohexane (C_6H_{12}). Cyclohexane, reagent grade, was purchased from Matheson, Coleman, and Bell, a Division of the Matheson Company, Incorporated, East Rutherford, New Jersey.
9. Graphite (C). Reactor grade graphite was used to fabricate the hot press dies and punches.
10. Molybdenum (Mo). The molybdenum sheet (0.010 inch) used for graphite die and punch liners and crucibles was obtained from the Fansteel Metallurgical Corporation, North Chicago, Illinois.
11. Miscellaneous. Various reagents and solvents commonly available in the laboratory were used during the cleaning and processing of specimens. Standard Buehler metallographic grinding and polishing materials were used for sample preparation.

Equipment

An induction-heated, horizontal, tube-type vacuum furnace and three different vacuum hot-press furnaces were used in this investigation. All of the furnaces were connected by appropriate fittings, valves, and bellows to conventional diffusion and mechanical vacuum pumping systems.

The horizontal-tube furnace, shown in Figure 4, consisted of a fused silica tube (four feet long, four inches inside diameter, three-eighths-inch wall thickness) supported by one-quarter-inch Transite panels. The ends of the fused silica tube were polished on 200 B grit Alundum to provide a sealing surface. The ends of the tube were closed with brass plates (nine inches in diameter, three-quarters-inch thick) provided with internal water coolant passages, and fittings for vacuum measuring instruments. The closure nearest the vacuum system was connected through a bronze bellows to the main vacuum valve. The closure at the front of the furnace contained a one-inch diameter pyrex sight glass clamped between rubber ring seals. The end plates were supported by three threaded aluminum rods (four feet long, three-eighths-inch diameter) which also served to clamp the end plates to the silica tube until a vacuum was established in the furnace. Sealing was effected by means of rubber rings and a thin film of high-vacuum grease.

A reactor-grade graphite tube susceptor (thirty-two inches long, two-and-one-eighth inches inside diameter, one-quarter-inch wall thickness) was supported concentrically in the silica tube by machined graphite rings. The annulus formed by the two tubes was loosely packed with carbon black for radial insulation. In the end of the susceptor tube nearest the vacuum pumps, two machined graphite heat shields, each consisting of four staggered plates, were set approximately two inches apart. Similar shields were located at the other end of the susceptor after each loading. The front shields had an axial hole, approximately one-half-inch in diameter, to permit sighting on the specimens. Adjacent to each

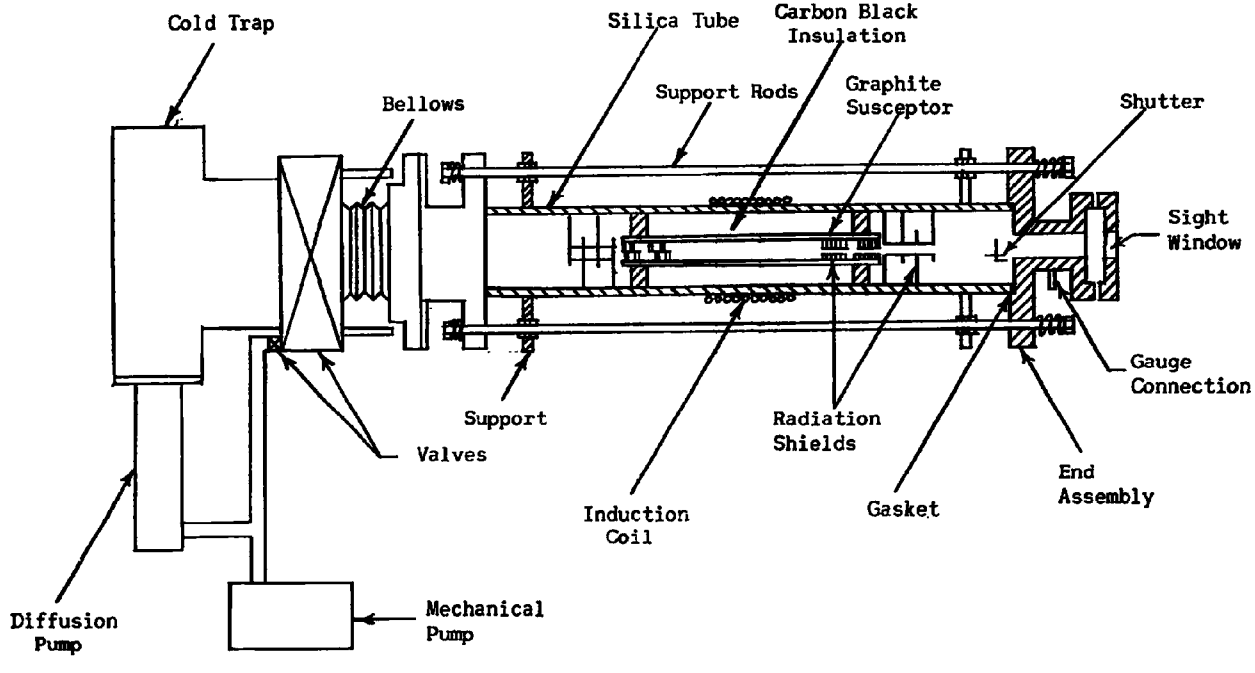

Figure 4. Partial cut-away diagram of the horizontal vacuum-sintering furnace

end and touching the susceptor was the last set of heat shields. Each consisted of six staggered semi-disks of 20-gauge steel spaced about one inch apart and bolted together. Again, the front shield assembly had an axial hole, three-quarters of an inch in diameter, to permit sighting into the reaction zone.

The furnace was heated with a water-cooled induction coil consisting of fifteen turns of one-quarter-inch copper tubing energized by a fifteen-kilowatt spark-gap generator.[1] The coil provided a hot zone approximately eight inches long at the mid-point of the susceptor tube. Within a two-inch central zone the temperature variation did not exceed 10°C. The generator was controllable through a percentage timer which could be preset to operate the unit for any selected fraction of each minute, from fifteen to one hundred per cent.

Temperature measurements were made with a Leeds and Northrup[2] disappearing-filament optical pyrometer. Vacuum measurements were made using a cold-cathode discharge tube[3] and a thermocouple tube[4] installed at each end of the furnace tube. The vacuum instruments were calibrated against a McLeod gauge with a range of 0.01 to 200 microns of mercury.

---

[1]Lepel High Frequency Laboratories, Incorporated, Woodside, New York.

[2]Model 8626-C, Leeds and Northrup Company, Philadelphia, Pennsylvania.

[3]Type GPH-100A, Consolidated Vacuum Corporation, Arlington, Virginia.

[4]Type GCT-3, Kinney Vacuum Division of the New York Air Brake Company, New York, New York.

The original vacuum hot press, shown in Figure 5, consisted of a fused silica tube (ten inches long, four inches inside diameter, three-eighths-inch wall thickness) supported vertically between two steel plates. An inner tube of mullite (ten inches long, two inches inside diameter, one-eighth-inch wall thickness) was supported concentrically by machined graphite rings. The annulus formed by the two tubes was loosely packed with carbon black for thermal insulation. The ends of the silica tube were polished on 200 B grit Alundum to provide a sealing surface. The lower steel plate, connected directly to the vacuum system, supported an alumina cylinder (three inches long, two inches in diameter) and an axial thermocouple. The upper plate assembly consisted of two parallel plates, the top one welded to a steel piston (four inches long, two inches in diameter). The bottom plate had an axial hole, sealed by a greased O-ring, through which the piston could travel. Flat rubber rings and high vacuum grease were used to seal joints between the steel plates and the silica tube. Both upper and lower plates were water-cooled by two turns of one-quarter-inch copper tubing attached to the edges of the plates.

The graphite die itself (three inches long, two inches in diameter) formed the susceptor. It was supported between cast alumina cylinders (three inches long, two inches in diameter) within the mullite tube.

Compacting pressure was provided by a Blackhawk[5] hydraulic ram, installed on a standard press frame. Pressure was transmitted through

---

[5]Proto-Power, Blackhawk Manufacturing Company, Milwaukee, Wisconsin.

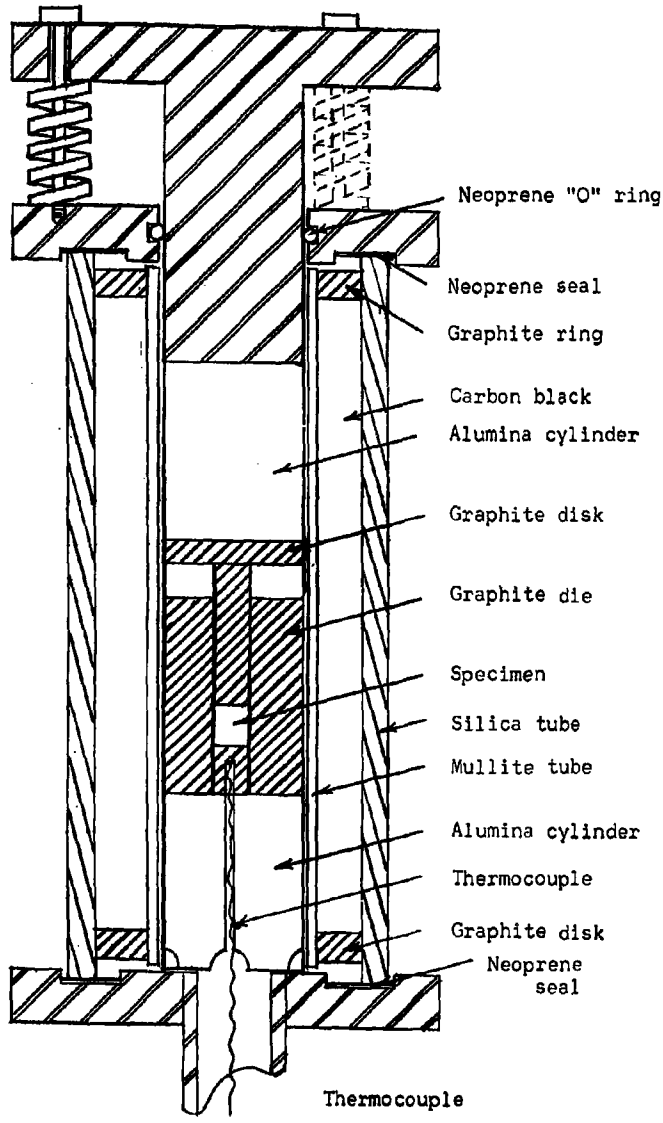

Figure 5. Cross-section of the vertical hot press

a steel ball joint to the upper plate assembly and thence through the alumina cylinders to the die punches. Die pressure calibration was based on physical dimensions of the system and indicated ram pressure.

Temperature measurements were made using a chromel-alumel thermocouple installed on the axis of the lower die punch, and located one-eighth-inch below the specimens. Calibration of specimen temperature vs. thermocouple temperature was accomplished using a second thermocouple imbedded in a UO_2 powder sample in the die cavity. Temperature measurements were made using a precision potentiometer.

Vacuum thermocouple tubes installed in the upper plate assembly and vacuum manifold, and a cold-cathode discharge tube installed in the vacuum manifold were used to obtain all vacuum measurements. The graphite die was heated by an eight-turn induction coil of one-quarter-inch copper tubing surrounding the fused silica tube. The coil, energized by a fifteen-kilowatt sparkgap generator, provided a uniform hot zone approximately one inch long at the mid-point of the die.

The second vacuum hot-press furnace, shown in Figures 6 and 7, consisted of a flanged steel pipe tee (four inches inside diameter, eight inches long) with an upper bellows assembly. The furnace body was cooled by one-quarter-inch copper tubing wrapped and brazed on its outer surface. One end of the tee was connected through flanged bellows to the vacuum manifold. The opposite end of the furnace had a pyrex glass (five inches in diameter, five-eighths-inch thick) closure through which the leads of the induction coil were passed. The upper bellows assembly supported and guided an alumina piston (two inches in diameter, eight

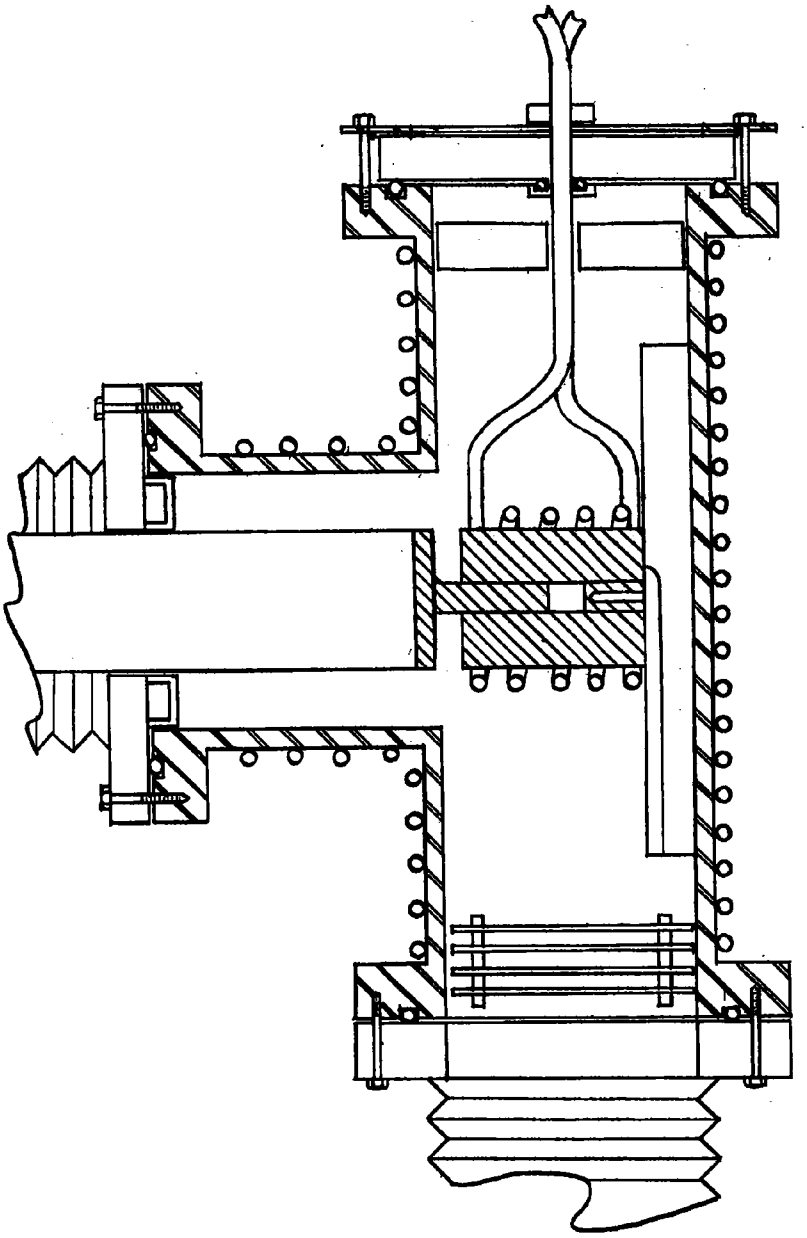

Figure 6. Partial cross-section of "Tee" vacuum hot press

Figure 7. Vacuum hot press and associated instrumentation

inches long) through which die pressures were applied. The graphite die (two inches in diameter, two-and-seven-eighths inches long) supported on a cast alumina block, formed the susceptor for heating. A five-turn water-cooled coil, formed from one-quarter inch copper tubing, was insulated from the die by sheet mica. The coil was energized by a fifteen-kilowatt spark-gap generator.

All vacuum seals were formed by greased O-rings installed within the connecting flanges. The bronze bellows permitted minor furnace movement and compacting pressure transmission while maintaining high vacuums in the system. Vacuum thermocouple tubes and cold-cathode discharge tubes were installed in both the furnace body and vacuum manifold. All gauges were calibrated using a McLeod gauge with a range of 0.01 to 200 microns of mercury.

Compacting pressure was applied by a Blackhawk hydraulic ram through a steel ball joint to the upper bellows assembly. Pressure transmitted by the alumina cylinder was applied to the top punch (one-half-inch diameter, two inches long) through a graphite disk (one-quarter-inch thick, two inches in diameter). A maximum die pressure of 4000 pounds per square inch was used to prevent rupture of the graphite die and punches at the firing temperature. Infrequent punch failures indicated that this was the limiting pressure for the configurations used.

Heat shields, fabricated from staggered half-disks of 20-gauge steel, spaced one-quarter-inch apart, were initially installed at both ends of the furnace. The front shields had to be replaced by a

one-half-inch disk of firebrick because the inductive field between the coil leads caused excessive heating and power loss in the metal shields.

Temperature measurements were made using chromel-alumel and platinum -10 per cent platinum-rhodium thermocouples connected to a precision Leeds and Northrup[6] galvanometric potentiometer. The thermocouple was located in a blind hole on the axis of the lower punch, with the thermocouple bead approximately one-eighth of an inch below the specimen. A second thermocouple, imbedded in UO_2 at the sample position correlated temperature readings to within 2°C during the initial furnace calibration.

The third vacuum hot press used was a standard Instron[7] tensile-testing machine fitted with a Richard Brew[8] high temperature, high-vacuum furnace. The resistance heated, clamshell-type tantalum elements would permit operating temperatures up to 2500°C in vacuums to 10^{-4} micron of mercury. Compressive loading was accomplished through O-ring-sealed ball joints in the furnace shell. Die pressures were controlled by means of a factory calibrated load cell installed as part of the Instron equipment. Temperature measurements were made with a chromel-alumel thermocouple installed in a blind hole drilled parallel and adjacent to the die cavity. The thermocouple bead was located approximately one-quarter-inch from the specimen. Optical pyrometer checks agreed within 5°C at firing temperatures with the thermocouple readings.

---

[6]Leeds and Northrup Company, Philadelphia, Pennsylvania.

[7]Model TTCLM, 10,000 pound capacity with reverse stress adjustment, Instron Equipment Company, Wilmington, Delaware.

[8]Richard D. Brew, Incorporated, 90 Airport Road, Concord, New Hampshire.

Two conventional inert-atmosphere glove[9] boxes were used to prepare handle and store sample powders. The boxes were kept filled with dry argon to minimize oxidation or contamination of the highly pyrophoric powders of UC and UH_3.

The x-ray equipment consisted of a Norelco[10] diffraction unit and high angle goniometer equipped with a scintillation counter, all of which was synchronized with an electronic chart-recording unit. All x-ray diffraction data were obtained using copper $K_{\alpha 1}$ radiation with nickel filters.

The metallographic work was done on a Bausch and Lomb research model metallograph, equipped for high magnification photomicrographic studies. Sample preparation was accomplished using conventional Buehler mounting and polishing equipment.

Other miscellaenous equipment included a Lindberg carbon-determination-type furnace, small, hardened steel ball mills (two inches inside diameter, six inches long), a 20-ton hydraulic press with steel punches and dies for making pellets, and the usual laboratory glassware and appliances.

Techniques

Production of Uranium Hydride. All of the uranium hydride used in the investigation was made in this laboratory by reacting clean uranium metal chips with dry hydrogen gas. Approximately one hundred grams of chips were reacted to produce each batch of hydride. The chips were

---

[9]CBR Model, Kewaunee Scientific Equipment, Adrian, Michigan.

[10]North American Phillips Company, Incorporated, Mount Vernon, New York.

first degreased by washing repeatedly in carbon tetrachloride and acetone. They were then pickled in boiling dilute nitric acid until bright and rewashed quickly in warm distilled water and acetone. The wet chips were then packed into a mullite reaction tube (eight inches long, one inch outside diameter) and the tube was loosely closed by tapered alumina plugs in each end.

The reaction tube was inserted into a larger mullite furnace tube installed in the Lindberg furnace. Most of the acetone was removed by evacuating the tube. A bubble counter, containing diffusion pump oil, was located at the furnace tube outlet to indicate gas flow. When drying was completed, the vacuum was broken with argon and the furnace tube subsequently maintained at a slightly positive argon pressure to avoid leakage of air into the tube.

The furnace was turned on, and as the temperature rose past 100°C, the argon gas flow was replaced by dry hydrogen gas. Care was taken to maintain a positive flow of hydrogen while the furnace temperature was being stabilized at 225-250°C. The reaction temperature was maintained for at least one hour, even though the hydriding reaction appeared to have been completed during the first few minutes, as indicated by the decrease in hydrogen consumption. The longer time was used to insure that the reaction was complete. When the furnace cooled to about 100°C, the hydrogen gas was replaced by argon and the furnace allowed to cool overnight to room temperature.

At the outset of the investigation, the cooled uranium hydride powder was unloaded from the reaction tube into an acetone-filled beaker.

The mild reaction that occurred with traces of moisture in the acetone passivated the powder by forming a uranium dioxide surface film. Although the powder so processed became reasonably stable for further handling in air, an undesirably high level of uranium dioxide was formed. The use of benzene and carbon tetrachloride in place of acetone resulted in less surface oxidation, but the dried hydride powders so produced remained slightly pyrophoric and unstable during storage. Since the hydride had to be handled and stored in an inert atmosphere, completely dry handling was attempted and used successfully throughout the remainder of the investigation. The hydride powder was produced in approximately one-hundred-gram batches as required, screened through a 200-mesh screen to remove any unreacted foreign material, and stored in the glove boxes until used. An x-ray diffraction analysis was made of each batch immediately after production, and only those which had an estimated impurity content, usually of uranium dioxide, of less than three per cent were used for further studies.

Preparation of Batch Compositions. The ingredients of each batch composition were weighed in the glove box to the nearest hundredth of a gram. They were then loaded into a clean steel ball mill with approximately one pound of mixed steel balls and sufficient reagent cyclohexaphen to half-fill the mill cavity. The ball charge consisted of equal parts of one-eighth, one-quarter, and three-eighths-inch steel ball bearings. Acetone, benzene, and carbon tetrachloride were initially tried as milling fluids, but cyclohexane was finally selected because the solubility of water in cyclohexane is virtually zero. Even small

percentages of water in the milling fluid reacted to produce undesirable oxidation when the powders were milled to extremely small particle sizes.

The milled slurries were unloaded in the glove boxes and allowed to settle for decanting of excess liquid. Up to six weight per cent of naphthalene was then dissolved in the resulting slurry and thoroughly mixed with the ingredients. Flowing argon was used to evaporate the remaining solvent while the batch was stirred constantly to distribute the binder uniformly. The dry powder was then stored in capped glass bottles until used.

Initially the uranium hydride and uranium monocarbide were milled simultaneously, but this procedure resulted in the oxidation of almost half of the hydride. It could not be determined whether the oxide was being formed only as a surface coating or if complete hydride grains were being reacted to form the oxide. X-ray diffraction analyses of the powders indicated that the uranium carbide contents were comparable to those introduced into the mill, while only half of the expected hydride content was found, the other half having been converted to uranium dioxide. Pure hydride, milled in cyclohexane both with and without milling agents, similarly was converted to equal parts of hydride and dioxide.

It was found that this problem could be avoided by premilling the uranium carbide with the milling agent in cyclohexane, and subsequently dry mixing the already finely-divided hydride with the milled carbide. X-ray diffraction analyses of the milled carbide powder indicated the presence of two to four per cent of uranium dioxide and up to six per cent of uranium dicarbide, both of which were probably in the powder prior

to milling. Grinding of the carbide for about fifty hours appeared to provide sub-micron powder. A very small percentage, two to three per cent as estimated microscopically, of the powder remained as large particles, from one to three microns in average diameter. Extending the milling time to one hundred hours did not eliminate the small amount of large particles.

It was found that three weight per cent of stearic acid, used as the milling agent, was sufficient to protect the batch powders against rapid oxidation. Naphthalene additions were, therefore, discontinued for the last fifteen batches. The powders so produced did not exhibit any pyrophoric tendencies when pressed into pellets or loaded into graphite dies during the short times they were exposed to room atmospheres.

Hand mixing of the carbide and hydride powders was attempted, but the fired specimens had gross segregation. It was found that two hours of dry mixing in argon was necessary and adequate to obtain a homogeneous powder. Specimens prepared from the dry-milled powders showed little segregation after firing.

Batch compositions with carbide contents from forty to seventy-five volume per cent were investigated. The uranium metal content, as reflected by the hydride contents, was slowly increased in an attempt to form a continuous uranium metal matrix while avoiding the formation of large lakes of uranium metal. Any such large lakes would exhibit the usual characteristics of massive uranium under irradiation and lose the dispersion-strengthening effect of the carbide grains. This range of compositions includes that of fifty atomic per cent of uranium metal, reported by

Kalish and Litton (25) to be essential to obtain bulk densities approaching theoretical.

Cold Pressing and Vacuum Sintering. Selected batch compositions were weighed and loaded into a double-acting hardened steel die in the glove boxes. Approximately six gram samples of powder provided specimen pellets three-eighths-inch in diameter by one-half-inch long. The die was enclosed in an argon-filled polyethylene bag for pressing in a twenty-ton capacity hydraulic press. Folded paper tissue was used to prevent tears in the plastic bag during pressing. Pellets were pressed for five minutes at pressures ranging from 19,650 to 100,000 pounds per square inch. The green pellets were extracted from the die within the polyethylene bag, and subsequently unloaded and stored in the glove box until ready for furnace loading.

The pellets, usually three per firing, were placed in individual molybdenum crucibles, five-eighths-inch in diameter and three-eighths-inch deep, fabricated from 0.010-inch-thick sheet. The crucibles were then placed on a stepped graphite boat, quickly loaded into the horizontal furnace and positioned in the hot-zone region. After replacing the front heat shields, the furnace was closed and evacuated to 0.05 micron. The specimens were then heated slowly by intermittently energizing the spark-gap generator. Slow initial heating was mandatory to avoid catastrophic rupture of the pellets by internally generated gas pressure during the critical degassing periods.

Critical degassing temperatures were determined by observing the behavior of pelletized specimens in a pyrex-tube furnace assembled for this purpose. A one-inch-diameter pyrex tube, about two feet long, was

connected directly to a high-capacity mechanical vacuum pump. Nichrome heater wire, wrapped around a four-inch mid-length of the tube, and powered through a Variac controller, provided a small controllable heat zone. A chromel-alumel thermocouple, inserted through the connecting vacuum hose, and located so that the specimen was in direct contact with the bead, was used to measure the specimen temperature. A vacuum thermocouple gauge was inserted through a rubber stopper and plugged into the other end of the pyrex tube to provide pressure measurements.

Samples of uranium hydride, uranium monocarbide, and prepared batches of the two constituents were inserted in the tube and slowly heated. Direct observation of the pellets permitted an accurate determination of the vacuum pressure variations at the temperatures where the highest degassing rates occurred. These temperatures were found to be approximately 100°C and 250°C. When the horizontal vacuum furnace was used, where only optical pyrometric temperature measurements could be made, the vacuum pressure variations were used to control the power input to the furnace during degassing. At the critical degassing temperatures, the relatively large changes in pressure corresponding to small changes in temperature provided a sensitive method of degassing control.

Very long degassing times, from four to eight hours of slow heating, were required to raise the specimen temperatures to about 600°C without exceeding a furnace pressure of one micron. If the heating rate was increased, particularly during the initial stages, complete pellet disintegration occurred with an accompanying sharp rise in furnace pressure to 200 or 300 microns. The firing was usually terminated whenever a

specimen disintegrated as a result of the too-rapid release of gas. This was either adsorbed gas, or gas formed by the decomposition of the binder.

Firing temperatures were determined by optical pyrometric sightings directly on the portions of the samples projecting above the crucibles. Temperature corrections for sight glass losses were made following each firing. The pyrometer was calibrated at the factory and frequently checked by comparison with a similar instrument using a tungste filament light source. The optical pyrometer was also calibrated against thermocouple measurements made in connection with another phase of this investigation.

After holding the specimens at the sintering temperature for the desired time, the spark-gap generator was turned off and the specimens were allowed to furnace-cool to room temperature before unloading. The typical furnace-cooling rate is shown in Figure 8. The cooled specimens were quickly removed from the furnace and inserted into the argon-filled glove boxes for preliminary investigation.

Hot Pressing. Selected batch compositions were weighed and loaded as powder into reactor-grade graphite dies. Ten-gram samples resulted in fired specimens one-half-inch in diameter and approximately one-quarter-inch long.

In most instances, the dies were fitted with molybdenum liners to avoid carbonization of the uranium metal formed during firing. Split

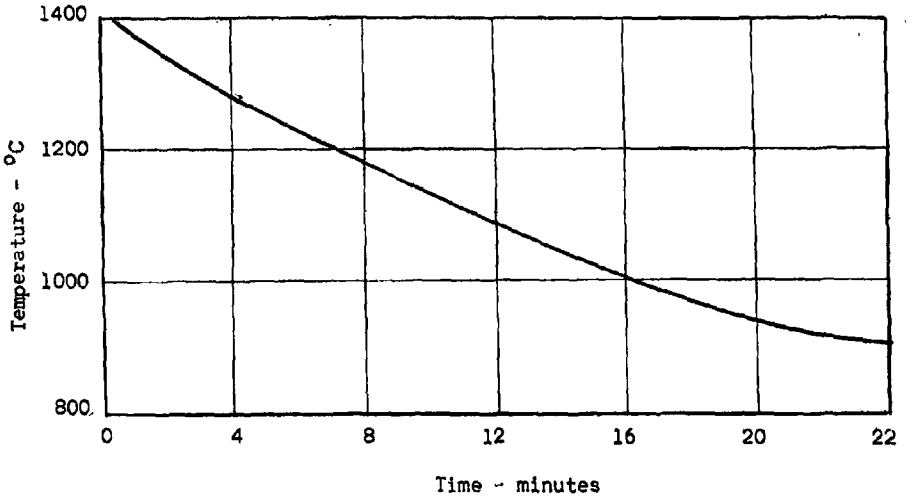

Figure 8. Typical horizontal furnace cooling curve

cylindrical sleeves were formed cold by hammering 0.010-inch sheet molybdenum around a hardened steel dowel pin using a split steel die. Disks used as punch facings were cut and filed to size manually. The die or liner surfaces were covered with a thin coating of alumina to minimize the Mo-U reaction which occurred at firing temperatures above 1200°C.

The filled dies were quickly loaded into the furnaces, thermocouples installed, and the furnaces evacuated to below one micron. The specimen powders were degassed by slowly raising the temperature while maintaining vacuums of less than one micron. Degassing could normally be completed within approximately two hours. The specimen temperature was subsequently raised to about 800°C, at which time the desired compacting pressure, from one to two tons per square inch, was applied. The specimen was then raised to the firing temperature while maintaining a constant compacting pressure. Softening and melting of the uranium metal could be detected by a rapid drop in die pressure.

After the desired time at temperature, the furnace power was cut off, and the specimens were allowed to furnace cool to room temperature. Figure 9 shows representative cooling rate curves of the samples taken from thermocouple data. From the curves it can be seen that the initial cooling rates are so high that the samples were practically quenched to temperatures below 1132°C, the melting point of uranium.

The specimens were allowed to cool in vacuum to room temperature before unloading. Considerable difficulty was encountered in extracting

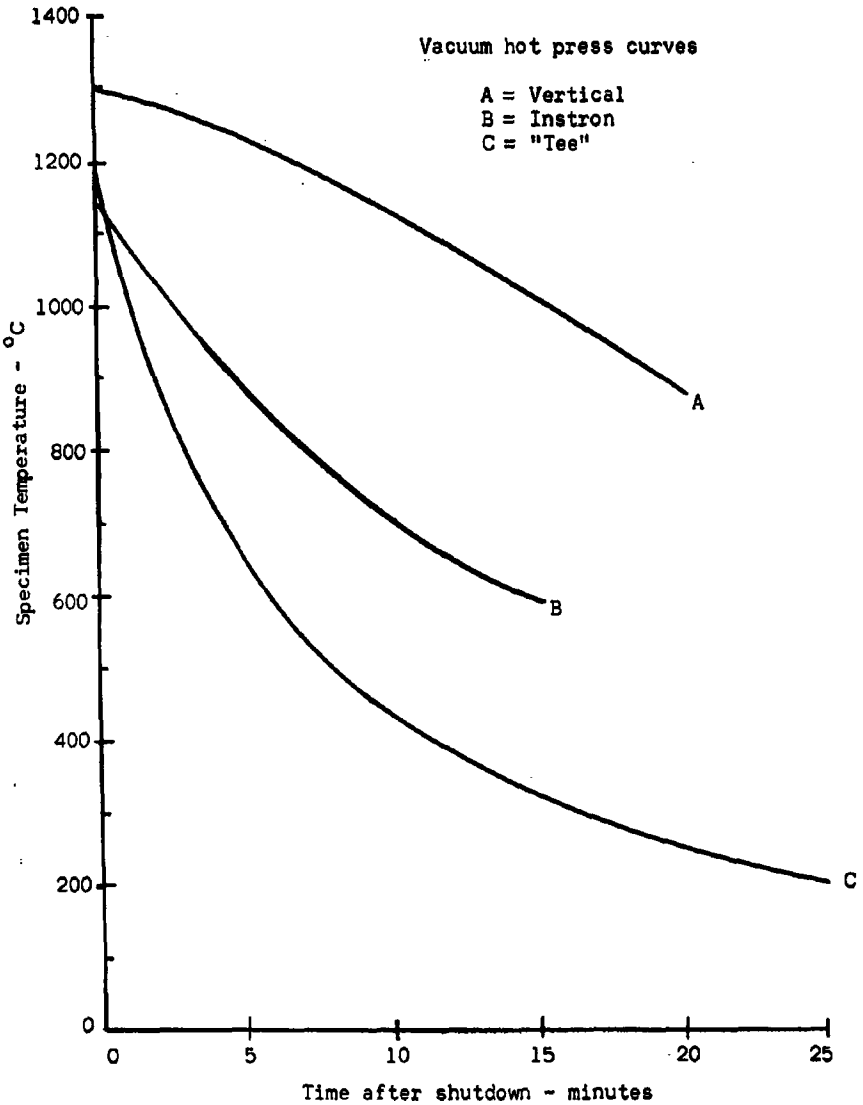

Figure 9. Hot press cooling rate curves

samples from the dies after firing above 1200°C. Occurrence of the Mo-U reaction necessitated destruction of the Mo liner to obtain the specimen.

The initial investigations were carried out in a hastily designed and built hot press previously described. The poor vacuum system geometry and high leak rate permitted excessive oxidation of the samples. The "Tee" vacuum hot press was then designed and built to provide improved vacuum, temperature, and pressure control. Near the end of the study an Instron tensile test machine equipped with a vacuum hot press was used.

Density Measurements. Bulk density measurements were made in two ways. A rough figure was obtained using measured weights, and volumes calculated from micrometer measurements. The reported values were obtained by the standard American Society for Testing Materials (ASTM) procedure using distilled water as the immersion medium.

X-ray Analysis. Powder samples for x-ray analysis were mounted in standard aluminum holders for the Norelco goniometer attachment. To prevent spillage or atmospheric reaction of the powders, they were coated with an acrylic spray called "Krylon Crystal Clear"[11] after mounting.

Pellet samples were ground flat on standard 1-0 metallographic paper and mounted in aluminum holders with modeling clay. Some pellets mounted in Bakelite for metallographic examination, were also held in place with clay.

---

[11]"Krylon Crystal Clear," acrylic spray manufactured by Krylon, Incorporated, Norristown, Pennsylvania.

All of the x-ray diffraction analyses were made using copper radiation filtered through nickel. The goniometer-mounted scintillation counter and the recorder were operated at two degrees per minute. Hanawalt files and standard sample charts were used in the evaluation of the analyses.

Metallographic Techniques. Specimens selected for metallurgical analysis were mounted in Bakelite mounts, ground flat on 200-grit silicon carbide paper with water coolant, and polished through 4-0 metallographic paper wetted with filtered kerosene. The final polish was obtained using Linde A alumina in kerosene as an abrasive on a Microcloth-covered polishing wheel. Light pressures minimized smearing of the uranium matrix or pull out of the carbide particles.

A number of etchants were tried, and the one that proved most satisfactory was a mixture with equal parts of concentrated nitric acid, phosphoric acid, glacial acetic acid, and distilled water. The samples were washed with acetone, etched 5 to 10 seconds, stopped with distilled water, rewashed with acetone, and blown dry in an air blast. Although the surfaces appear stained, under magnification the uranium metal appears bright yellow, the uranium monocarbide orange, the uranium dioxide gray, and voids are completely black. Good definition of particles less than one micron in diameter was obtained. Examination at 2125X magnification using oil immersion was necessary to see the grains in the samples that had the desired microstructure. Particle size was determined with a Fowler eyepiece which was calibrated with a scribed plate. The photomicrographs were all taken at 2000X magnification.

A grid-counting method similar to that proposed by Hilliard and Cahn (22) was used to determine the amount of porosity and to check

x-ray compositional analyses. The published technique was modified for direct counting on etched specimens. The intersection of the hairlines in a calibrated Fowler eyepiece was used to establish each counting point of the grid. The specimen surface was traversed with the hairlines at uniform intervals in two perpendicular directions. The grid interval for a specimen was between 2 and 10 microns, depending on the average grain size in the specimen. The phase (or porosity) observed at each preset grid point was recorded for at least 500 grid points. The relative number of points at which a given phase (or porosity) was observed indicated the volume fraction of that phase in the specimen. The relative standard deviation of the volume fraction of a phase due to the counting error was cited to be $1/\sqrt{N_p}$, where N_p is the number of points falling on the phase being determined (22).

RESULTS AND DISCUSSION

Cold Pressing and Vacuum Sintering

Specimens containing varying percentages of uranium carbide were fired at temperatures up to 1500°C in both vacuum and argon atmospheres. At firing temperatures below 1100°C, the specimens exhibited little or no shrinkage, had high porosity, and in every case spontaneously ignited and burned if exposed to the room atmosphere for just a few minutes. These samples apparently had not sintered, and the high connected void volume provided a large surface area for reaction since all of the protective binder had been removed during the firing. The specimens which were not allowed to burn were stored in the glove boxes and observed periodically. Within three weeks, all of the pellets had returned to a highly pyrophoric powder form. Specimens fired at temperatures in excess of 1132°C showed various degrees of sintering, depending on the time they were held at temperature. In every case, however, large pores were formed throughout the specimens, and very low bulk densities were obtained. The highest value attained was 11.26 grams per cubic centimeter, which for that sample was only 61 percent of the theoretical density calculated from its x-ray analysis. When additional uranium hydride was added to raise the uranium metal content, no significant change in the character of the porosity or density was obtained.

Microscopic examination of sintered samples at 250X magnification showed pores from 2 to 200 microns, distributed over the entire specimen surface. At higher magnifications, up to 2000X, the surfaces of

the pores appeared to consist completely of uranium dioxide. A mass spectrographic analysis of the gas evolved from similar test specimens showed an extremely high nitrogen concentration, with traces of argon. It is postulated that the oxygen in the air adsorbed by the powders before or during processing reacted with the highly active free uranium metal, releasing the nitrogen and argon detected by the analysis. The high concentration of uranium dioxide in the fired specimens was also reflected in x-ray diffraction analysis of the specimens.

An attempt was made to sinter at higher temperatures for very short times to improve the specimen density. The results are illustrated in Figure 10. Figure 10a shows the microstructure of the sample fired to 1200°C and immediately furnace-cooled. The largest particles visible are about two-and-one-half microns in diameter. The pores, which show as black spots on the photograph are seen to be distributed throughout the specimen. No uranium matrix structure is discernible, and the pellets fractured easily. When the sintering temperature was raised to 1370°C, the general grain growth that occurred is evident in Figure 10b. Each of the phases and the voids grew larger. No real improvement in density or strength was noticeable. As the temperature was raised further to 1485°C, grain growth proceeded as shown in Figure 10c. At this temperature, an increase in density was detectable, but the grain growth that occurred makes this approach valueless in view of the objectives of this investigation. Several subsequent firings corroborated these findings; and, as a result, further attempts using cold pressing and vacuum sintering were abandoned.

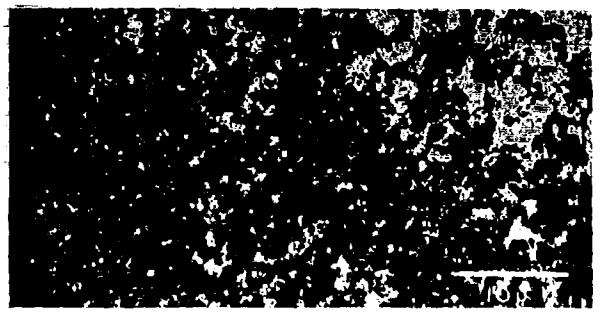

a. 1200°C 2000X

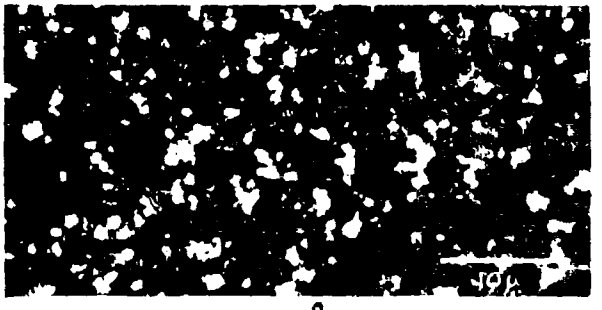

b. 1370°C 2000X

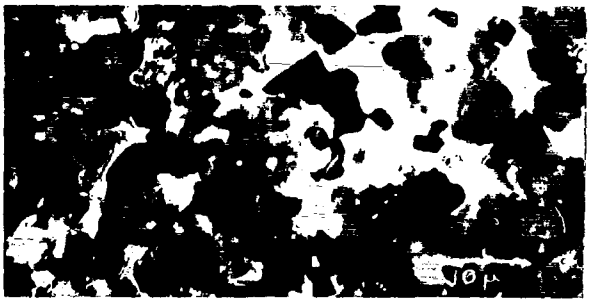

c. 1485°C 2000X

Figure 10. Microstructures of cold-pressed specimens as a function of sintering temperatures

A single attempt was made to cold-impact-press a specimen using a variable impact vibrator to obtain a much higher green pellet density. Great difficulty was experienced in extracting the pellet because the fine-milled powder moved into the small annular clearance between the die and punches. Only a small portion of the resulting pellet was obtained intact, but because of its much higher green density, it exploded to powder in the sintering furnace as soon as its temperature was raised. This approach might permit achieving the desired objective if the time and equipment were available to develop the pressing, extraction, and firing techniques.

Hot Pressing

The alternative technique of vacuum hot pressing was investigated in an attempt to obtain higher bulk densities without the undesirable grain growth experienced using cold pressing and vacuum sintering procedures. Although the first vacuum hot press used was relatively crude, the results obtained with it indicated that this approach was promising. Figures 11 and 12 illustrate the microstructures obtained during these initial experiments. In both cases the oxide contents were much too high, and little free uranium metal was detectable.

The firing times and temperatures at which hot-pressed specimens were studied are indicated by an "x" in Figure 13. The solid vertical bar associated with each firing condition indicates the range of grain sizes measured in a representative surface of the specimen. It can be seen in Figure 13 that at all firing temperatures above 1200°C significant grain growth occurred except in specimens 55 and 65. With these exceptions

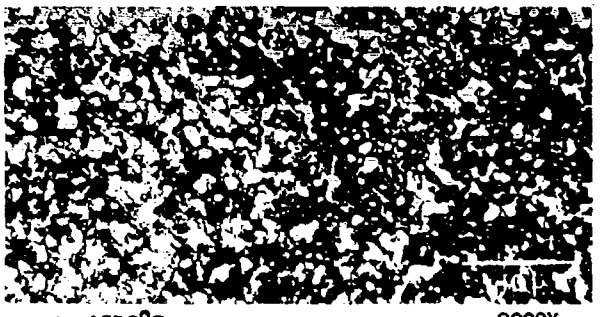

Figure 11. Microstructure of Specimen 55

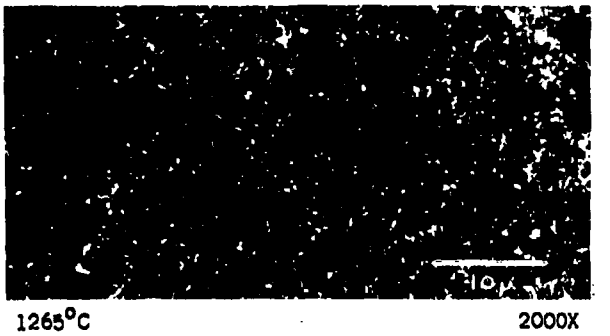

Figure 12. Microstructure of Specimen 65

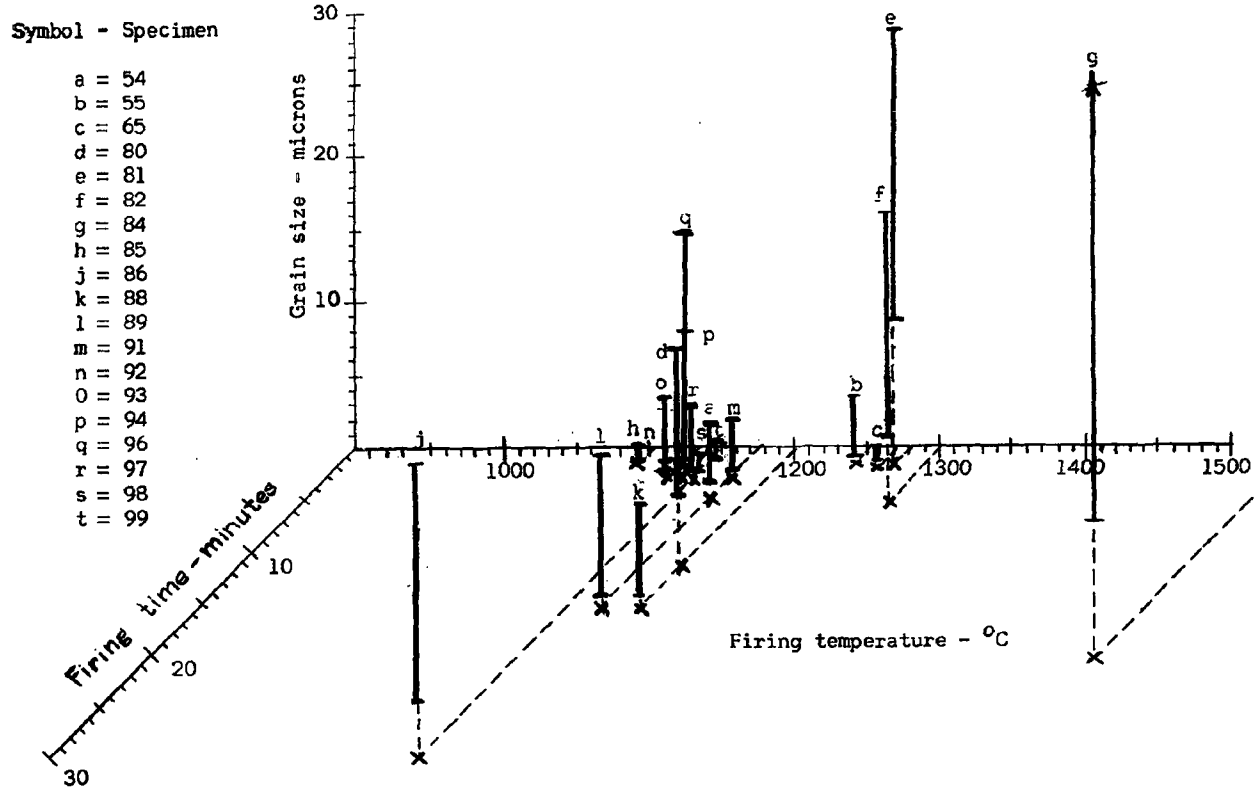

Figure 13. Hot press firing temperatures and times vs. grain sizes (900 - 1500°C)

grain sizes varied from at least four to thirty-five microns; no small grains were discernible. Specimens fired at these temperatures, even for times as short as a few seconds, had large recrystallized grains throughout the microstructure. The firing temperature of specimen number 55, Figure 11, was estimated to have reached only 1250°C after the thermocouple failed at 1120°C. The estimate was based on prior firing experience, but it is possible, and likely, that the specimen temperature never reached 1200°C. Its microstructure appears to be similar to that of samples fired at 1175-1200°C, indicating further that the firing temperature was probably within this range. Specimen 65, Figure 12, which was fired at 1265°C retained a fine-grained structure, but it was found to consist predominantly of uranium dioxide. Oxidation of the sample most likely occurred at low temperature, between 450 and 800°C, as the uranium hydride decomposed. The usual sharp pressure increase accompanying gross oxidation of the sample either did not occur, or it was undetected when it did occur. The presence of the high oxide concentration apparently retarded grain growth of the carbide phase by keeping the individual carbide grains widely separated. The probable action of uranium dioxide as a grain growth inhibitor is examined in detail in a later section of the discussion.

The specimens hot pressed at or below 1130°C did not appear to be fully sintered. Bulk densities of specimens fired in this temperature range never exceeded eighty per cent of theoretical. Specimens fired at or below 1104°C ignited and burned when they were exposed to the room atmosphere for a few minutes.

The two specimens nominally fired at 1130°C illustrate the different results obtained by solid and liquid phase sintering. The small uncertainty in the actual specimen temperature probably caused Specimen 92 to be fired slightly below the melting temperature of uranium while Specimen 93 was fired at slightly above 1132°C. Specimen 92, although it retained the originally small grain structure of the powder, had very low density (79 per cent of theoretical), and it oxidized rapidly when removed from the furnace. Specimen 93, in which the grain size was slightly larger (1 to 5.5 microns), had a density 96 per cent of theoretical. The large spherodized uranium carbide grains, formed during recrystallization even at such low temperatures, and the uranium metal matrix are shown in Figure 14. Isolated uranium dioxide grains, one micron and smaller, are distributed throughout the structure, and generally located adjacent to the uranium metal. Figure 15 expands the time-temperature region of Figure 13 that was most extensively investigated. Inspection of the figure indicates that long firing times (exceeding three minutes) and firing temperatures near 1200°C result in excessive grain growth. Specimens fired at temperatures between 1130 $\pm$ 5°C 1150 $\pm$ 5°C for times ranging from a few seconds to three minutes and at die pressures at 3500-4000 pounds per square inch approximated the desired microstructure. The exceptions, specimens 94 and 96, contained very low percentages of uranium dioxide, approximately 6 per cent, as compared to 10 to 15 per cent for the remaining specimens. The typical low oxide content and large grain size of these two specimens is shown in Figure 16. In contrast, Figure 17, illustrates the typical

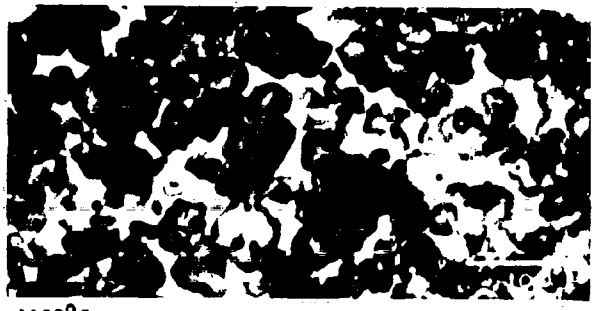

1132°C 2000X

Figure 14. Microstructure of Specimen 93

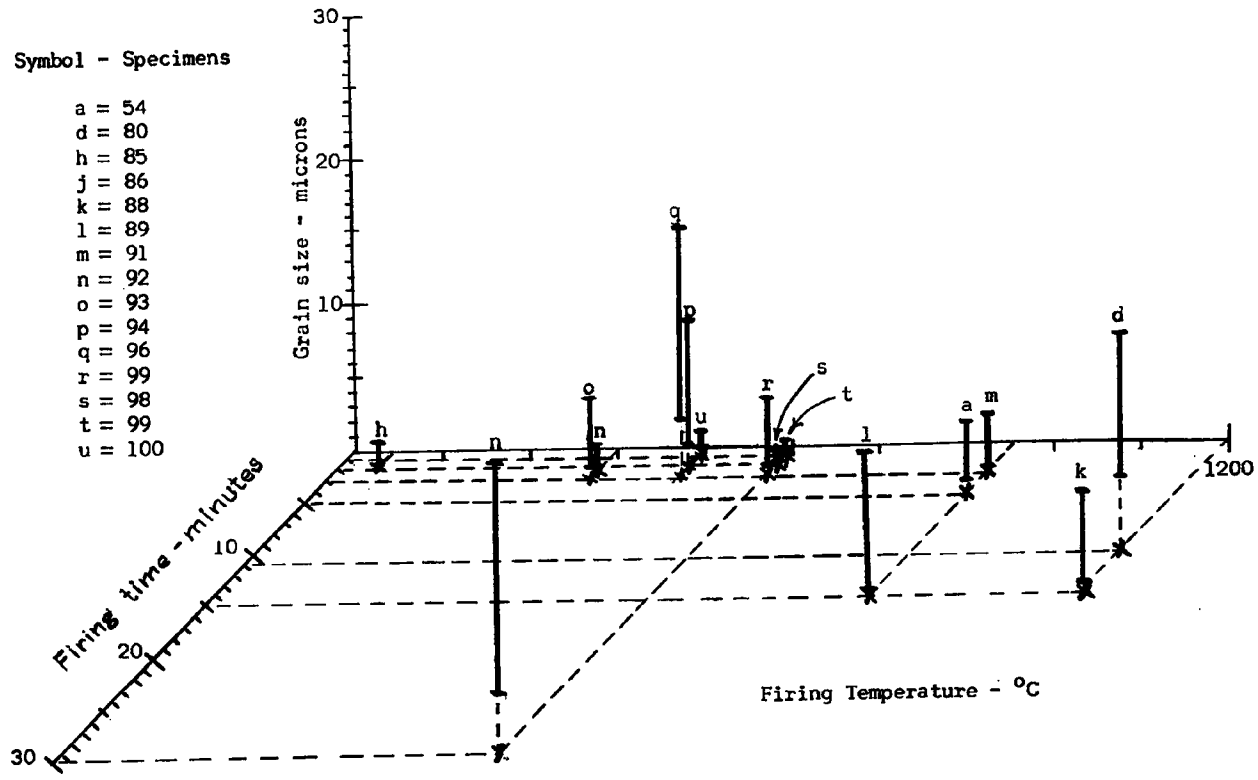

Figure 15. Hot press firing temperatures and times vs. grain sizes (1100-1200°C) - (Expanded section of Figure 13)

1140°C 2000X

Figure 16. Microstructure of Specimen 94, low oxide content (6%)

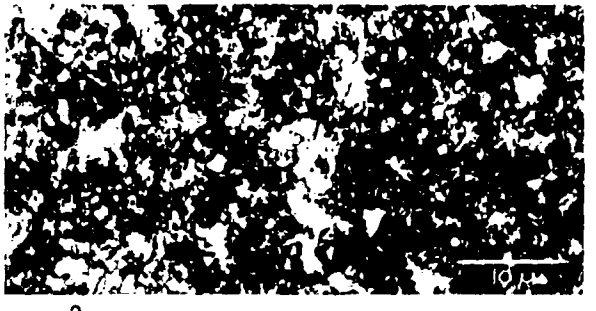

1150°C 2000X

Figure 17. Microstructure of Specimen 98, high oxide content (10-15%)

microstructure of those specimens with the slightly higher oxide content. The densities of the small-grained specimens varied between 93 and 96 per cent of theoretical density, based on x-ray and metallographic analyses of the samples.

Uranium Dioxide as Grain Growth Inhibitor

In the previous section some anomalous grain size results were noted. It is believed that uranium dioxide, when properly distributed, acts as a grain growth inhibitor for the uranium monocarbide. Low concentrations of uranium dioxide in high purity batch compositions, conversely do not provide this grain growth inhibition.

It was mentioned earlier in this discussion that high levels of surface oxidation of the uranium hydride powders were undesirable. Highly oxidized powders decreased the amount of uranium metal in the fired samples, lowered the overall density and thermal conductivity of the fuel material, and decreased the uranium atom density. The avoidance of any uranium dioxide contamination of the sample powders was initially considered to be the ultimate objective.

From the results of this investigation it is believed that a small amount, from 10 to 15 per cent, of uranium dioxide can act as an effective grain growth inhibitor for the uranium-uranium monocarbide fuel without seriously affecting the overall properties of the material. This range of UO_2 concentration generally agrees with that proposed in Arbiter's (2) Patent for dispersion hardening uranium metal, and is similar in effect to Vordahl's (52) technique for controlling grain size in other highly reactive metals and alloys.

It was established earlier that almost all of the oxide was formed by reaction of the hydride, either with air or moisture. If it is assumed that the oxide is formed principally as a surface coating on the fine hydride particles, rather than by complete oxidation of whole grains, then each particle would consist of a "skin" of oxide enclosing the hydride core. The behavior and microstructure of the specimens investigated appear to be influenced by the uranium dioxide concentration of the starting powders.

Role of Oxide in Cold Pressing and Vacuum Sintering. In a homogeneous mixture of carbide and surface oxidized hydride powders, the carbide grains would only "see" uranium dioxide. Cold pressing of such powders, even at high pressures, would probably result in only point contact between the carbide and hydride, as depicted in Figure 18a. According to Goetzel (14) the porosity of the green compacts theoretically could not be less than 26 volume per cent. It is probably much higher as a result of the imperfect packing of irregularly shaped grains and the small average grain size.

When such pellets are vacuum sintered without any externally applied pressure, particularly at the low temperature used in this investigation, very little densification occurs. During the initial phases of firing, when the hydride is decomposed and hydrogen gas removed from the powder, a small amount of shrinkage occurs as the low density hydride is replaced by the high density metal. Part of the internal stress imposed during pressing is relieved by the small decrease in volume.

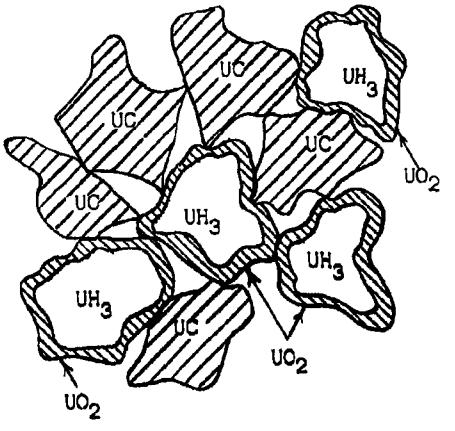

a. Room temperature

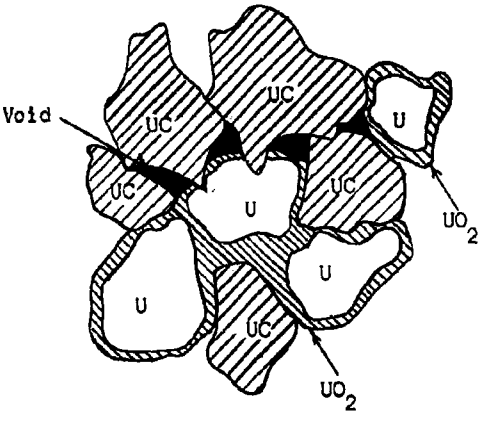

b. 800 - 1300°C

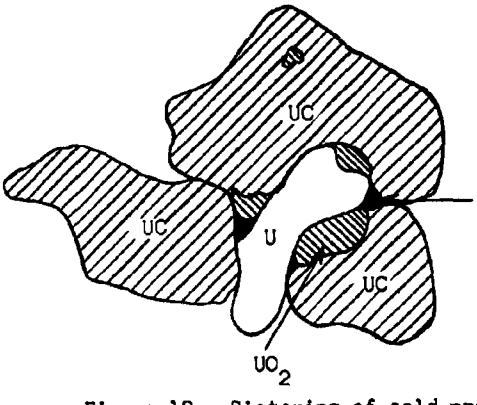

c. 1300°C

Figure 18. Sintering of cold pressed specimens

As the temperature is increased above 800°C and approaches the melting point of the uranium, the remaining stresses are probably relieved by plastic flow and distortion of the oxide encapsulated metal. When the temperature is increased further, the molten uranium appears to be retained within the oxide skin, which has far higher softening and melting temperatures. At temperatures between 1132°C and 1350°C, therefore, little grain growth should occur, and was so observed, because the oxide films prevent liquid phase sintering from taking place. Figure 18b depicts the microstructures observed for firings in this range of temperatures. The high distributed porosity results from the incomplete solid phase sintering of carbide and oxide at such low temperatures.

When the firing temperatures were raised above 1350°C, the increased thermal energy combined with the lower strength of the oxide led to rupture of the films and an increase in density as the freed uranium filled adjacent pores, and carbide grain growth proceeded at a high rate. Coarse-grained microstructures, such as is depicted in Figure 18c, were obtained at the higher sintering temperatures. Full densification was never achieved with the cold-pressed specimens because the high temperatures, where carbide-oxide sintering could occur, were never reached.

Dienst and Werner (10) found essentially the same effect when using any preoxidized powder. They found that the continuous oxide skeleton, a slow-sintering component retained in the body during sintering, essentially determined rate of sintering. Superficial layers of oxide decreased the thermal activation energy of the sintering mechanism up to 50 per cent in the case of copper and iron powders. Changes of at least

the same order of magnitude are expected for the highly surface-active materials used in this study.

Role of Oxide in Hot Pressing. The addition of externally applied stress during firing results in significant changes in the sintering process described in the previous section. Since pressure was applied to the specimens when the temperature reached approximately 800°C, the initial phase of the sintering process occurs as described earlier (Figure 19a). When the uranium metal approaches its melting point, the applied die pressures were sufficient to induce flow and rupture of the oxide films. The oxide was forced to the contours of the carbide grains immediately surrounding the original hydride particle, where the oxide was formed into small grains by the surface tension of the uranium as depicted in Figure 19b.

As the firing temperature reaches and exceeds the melting point of uranium, the molten metal penetrates between the adjacent carbide grains under hydrostatic, capillary, adherent, etc., forces (Figure 19c). The lubricating action of the molten metal may also assist in improved packing of the carbide grains. Even at temperatures slightly above the melting point of uranium, therefore, high bulk densities are attainable. At slightly higher temperatures, grain growth of the carbide proceeds at a rapid rate. The mobility of carbide atoms at the uranium wetted surfaces is extremely high, and spheriodization and growth of the carbide occurs in very short times.

In powders with low uranium dioxide concentrations, the amount of oxide available to act as barriers to carbide grain growth is insufficient

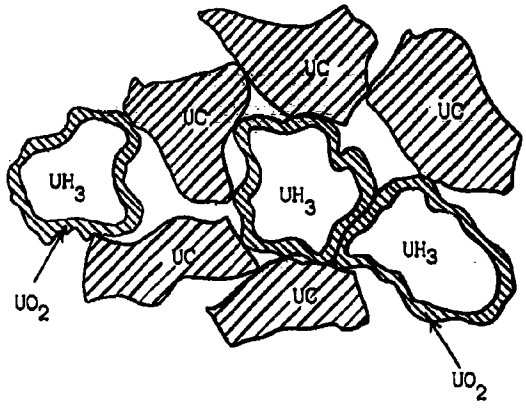

a. RT to 800°C

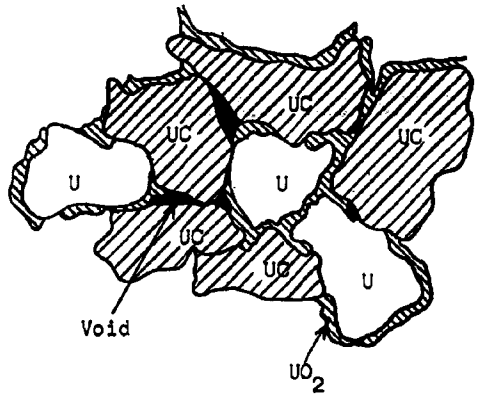

b. 800 - 1132°C

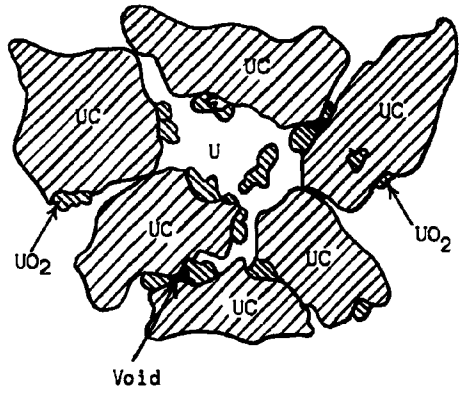

c. 1132°C

Figure 19. Sintering of hot pressed specimens

to prevent almost explosive growth. Specimens 94 and 96 exemplify the grain growth that occurs. The samples produced from powders with slightly higher oxide concentrations showed grain growth inhibition (Figure 17). Higher oxide concentrations inhibited carbide grain growth even at higher temperatures. The small grain size of Specimen 65 (Figure 12) is probably the result of such grain growth inhibition. When much higher temperatures or longer firing times are used, however, the inhibiting effect of the oxide phase is overcome by the driving force for growth of the fine carbide powders.

Although higher concentrations than ten to fifteen per cent of the oxide phase would be more effective as a growth inhibitor, the lowest possible uranium dioxide concentration was desired in the fuel element material under development. In order to obtain the desired microstructure, uranium dioxide concentrations of ten to fifteen per cent are considered acceptable. The dioxide, in the form of uniformly distributed particles, one micron or less in size, is not expected to lower the thermal or physical properties of the material very much. The short heat paths within the dioxide grains should preclude high central grain temperatures even at high reactor power levels. The small grain size should provide additional grain boundary discontinuities to promote fission gas nucleation sites. Only in-pile tests, however, can evaluate the possible detrimental effects of uranium dioxide additions to the fuel material under study.

SUMMARY

This investigation was undertaken because theoretical considerations and some experimental evidence indicated that a uniform dispersion of very small uranium monocarbide particles in a uranium matrix would be an outstanding nuclear fuel material. In the preparation of specimens, conventional powder metallurgical processing techniques had to be modified. For example, the powdered raw materials oxidized excessively when they were milled in the liquids normally used for this purpose. The best procedure for preventing oxidation consisted of milling only the uranium monocarbide powders in cyclohexane. After drying, the carbide was mixed with freshly prepared uranium hydride powder by dry milling for one or two hours. The resulting powders were then either cold-pressed and vacuum-sintered or hot-pressed at temperatures between 980°C and 1500°C.

Initially it was thought that the specimens should be as nearly free of oxide contamination as possible. However, uranium monocarbide particle growth was excessive except when as much as 10 to 15 per cent of finely dispersed uranium dioxide was present in the specimens. Under certain conditions the surfaces of the individual particles of uranium metal became coated with a layer of oxide. This generally occurred before the uranium hydride decomposed to form the metal. During hot-pressing, applied pressures of 3500 to 4000 psi cause the oxide films to rupture, and this permitted the molten metal to infiltrate between the uranium monocarbide grains. In this process the uranium dioxide

became uniformly distributed in the specimens. Cold-pressing and sintering did not produce dense specimens because the oxide films were not broken; and, when the particles of metal melted, the liquid metal remained encased in oxide. This effectively prevented liquid phase sintering, and the temperatures were not high enough for densification by solid state sintering.

Even when oxide was present during hot-pressing, time and temperature were of primary importance in controlling densification and uranium monocarbide particle growth. Specimens with the desired microstructure could be produced only by hot-pressing at temperatures between 1132°C (the melting point of uranium) and 1150°C for three minutes or less. Higher temperatures or longer times resulted in excessive uranium monocarbide particle growth and satisfactory densification was not obtained at lower temperatures.

CONCLUSIONS

A uranium-uranium monocarbide-uranium dioxide material which should be an outstanding nuclear fuel has been developed in this investigation. The unique microstructure of this material consisted of uranium monocarbide particles and, to a lesser extent, uranium dioxide particles three microns or less average diameter dispersed in a uranium matrix. A density of approximately 10^{10} particles per cubic centimeter was obtained. This should provide sufficient sites for nucleation of fission gas products so that small bubbles of these gases will form instead of large ones. In this case the "swelling," which limits the usefulness of uranium metal fuel elements, will be eliminated. The physical and nuclear properties of the uranium-uranium monocarbide-uranium dioxide material should also make it desirable for use as a nuclear fuel. Irradiation testing of this material is planned.

Vacuum hot pressing at 3500 psi between 1132 and 1150°C for three minutes or less was the most satisfactory technique for making specimens of the uranium-uranium monocarbide-uranium dioxide material. Uranium dioxide contents of 10 to 15 per cent by volume effectively inhibited uranium monocarbide grain growth provided that hot pressing temperatures and pressures were within the above limits.

LIST OF REFERENCES

1. Staff, Atomics International. 1962. Annual technical progress report. AEC unclassified programs, NAA-SR-7400.[12]

2. Arbiter, W. 1963. Dispersion hardening of uranium metal. U. S. Patent 3,073,698.[13]

3. Ball, J. G. 1960. Materials in atomic energy. Nuclear Power 2:79-90.

4. Barnes, R. A., and G. W. Greenwood. 1961. The effect of gases produced in reactor materials by irradiation. Progress in Nuclear Energy, Series V, Metallurgy and Fuels. Pergammon Press, New York.

5. Barnes, R. S. 1957. The formation of internal gas bubbles in solids. J. Nuc. Energy 5:301-319.

6. Binder, I., and R. Steinitz. 1959. An investigation of the mechanical properties of cermets as related to the microstructure. WADC Technical Report 58-432.[12]

7. Bolta, C., and A. Strasser. 1960. Carbide fuel development, Phase II report, period of September 15, 1959, to September 15, 1960. NDA-2145-6.[12]

8. Boltax, A. 1962. Behavior of fissionable material under irradiation, Nuclear reactor fuel elements. John Wiley and Sons, New York.

9. Chubb, W., and F. A. Rough. 1960. Research on uranium carbide and uranium carbide-base fuel materials at Battelle Memorial Institute. TID-7603.[12]

10. Dienst, W., and O. Werner. 1960. The sintering process in metal powders. Zeitschrift für Metallkunde 51:45-50.

11. Endebrock, R. W. (Ed.). 1962. Properties of fuels for high-temperature reactor concepts. BMI-1958.[12]

12. Finley, J. J., M. Korchynsky, and S. Sarian. 1960. Columbium alloy clad uranium carbide fuel element. Union Carbide Metals Company, Niagara Falls, New York.[12]

13. Goetzel, C. G. 1949. Treatise on powder metallurgy. Interscience Publishers, Inc. New York.

14. Goetzel, C. G. 1954. Method of manufacturing heat resistant sintered articles. U. S. Patent 2,852,367.[13]

15. Greenwood, G. W. 1959. Volume increases in fissile materials on neutron irradiation and the effects of thermal fluctuations. AERE-R-2864.[12]

16. Greenwood, G. W., A. J. E. Foreman, and D. E. Rimmer. 1959. The role of vacancies and dislocations in the nucleation and growth of gas bubbles in irradiated fissile material. AERE-R-2863.[12]

17. Griffiths, L. B. 1961. The effect of irradiation and post-irradiation annealing on the electrical resistivity of uranium monocarbide. J. of Nuc. Materials 4(3):336.

18. Hamme, J. V. 1963. Phase relationships in the uranium-carbon-oxygen system. Ph.D. dissertation, Department of Mineral Industries, North Carolina State College, Raleigh, North Carolina.

19. Hare, A. W., S. Alfant, F. A. Rough, and D. I. Sinizer. 1960. Further results of irradiation of uranium carbide. Trans. Am. Nuc. Soc. 3(1):133-134.

20. Hausner, H. H., and H. C. Friedemann. 1961. Bibliography on uranium carbides. NP-11407.[12]

21. Hayward, B. R. 1960. Study of irradiation damage in fuel materials at high temperature. NAA-SR-5350.[12]

22. Hilliard, J. E., and J. W. Cahn. 1961. An evaluation of procedure of quantitative metallography for volume-fraction analysis. Trans. AIME 221(2):344-352.

23. Holden, A. N. 1958. Physical metallurgy of uranium. Addison-Wesley Publishing Company, Inc. Reading, Massachusetts.

24. Kalish, H. S. 1961. The development of uranium carbide as a nuclear fuel. NYO-2694.[12]

25. Kalish, H. S., and F. B. Litton. 1960. Development of uranium carbide as a nuclear fuel at Olin Mathieson Chemical Corporation. TID-7603.[12]

26. Katz, J. J., and E. Rabinowitch. 1951. The chemistry of uranium. McGraw-Hill Book Company, Inc. New York.

27. Kaufmann, A. R. (Ed.). 1962. Nuclear reactor fuel elements-metallurgy and fabrication. John Wiley and Sons. New York.

28. Lloyd, H., and J. Williams. 1961. The powder metallurgy of uranium and its alloys. Progress in Nuclear Energy, Series V, Metallurgy and Fuels. Pergammon Press, New York.

29. McGeary, R. K. 1958. Oxide fuel elements. A forum committee report on reactor fuel technology. The Atomic Industrial Forum, Inc. New York.

30. Meyerson, G. A., R. B. Kotel'nikov, and S. N. Bashlykov. 1960. Uranium carbide. Atomnaya Energiya 9(5):387-391.

31. Murray, P. 1956. The hot pressing of ceramics, symposium on powder metallurgy. The Iron and Steel Institute, London.

32. Murray, P. 1957. Some aspects of ceramics in atomic energy. The Refractories Journal 33:2-6.

33. Nuclear engineering data sheet, No. 15, uranium carbide. 1960. Nuc. Engr. (London) 5:357.

34. Pidd, R. W. 1959. Characteristics of UC,ZrC, and (ZrC) (UC) as thermionic emitters. J. Appl. Phys. 30:1575-1578.

35. Power Reactor Technology 6(2):43-46. 196.[12]

36. Proceedings of the symposium on uranium carbides as reactor fuel materials held at Atomic Energy Commission Headquarters Building, Germantown, Maryland, April 4, 1961. TID-7614.[12]

37. Quatinez, M., R. J. Schafer, and C. Smeal. 1961. The production of submicron metal powders by ball-milling with grinding aids. Trans. Met. Soc. AIME 221:1105-1110.

38. Rogers, M. D., and J. Adam. 1962. Radiation damage and its thermal recovery in uranium monocarbide and uranium mononitride. AERE-R-4046.[12]

39. Rough, F. A., and W. Chubb. 1960. Progress relating to civilian applications during March 1960. BMI-1430.[12]

40. Rough, F. A., and W. Chubb. 1960. An evaluation of data on nuclear carbides. BMI-1441.[12]

41. Rough, F. A., and W. Chubb. 1960. Progress relating to civilian applications during September 1960. BMI-1469.[12]

42. Rough, F. A., and W. Chubb. 1961. Progress in the development of uranium carbide-type fuels, final report on the AEC fuel-cycle program. BMI-1554.[12]

43. Rough, F. A., and R. F. Dickerson. 1960. Uranium carbide, fuel of the future. Nucleonics 18:74-77.

44. Rough, F. A., A. W. Hare, R. B. Price, and S. Alfant. 1960. Irradiation of uranium monocarbide. Nuc. Sci. and Engr. 7(2):111-121.

45. Russell, L. E. 1963. The structure and properties of U-C and (UPu)-C alloys. AERE-R-4330.[12]

46. Schwarzkopf, P. 1947. Powder metallurgy. The Macmillan Company, New York.

47. Snyder, M. J., and A. B. Tripler. 1960. Some refractory uranium compounds. ASTM special technical publication No. 276. ASTM, Philadelphia, Pennsylvania.

48. Strasser, A. 1960. Uranium carbide as fuel, a review of current knowledge. Nuc. Engr. (London) 5(51):353-357.

49. Taylor, K. M., and C. H. McMurtry. 1961. Synthesis and fabrication of refractory uranium compounds. ORO-448.[12]

50. Taylor, K. M., and C. H. McMurtry. 1962. Synthesis and fabrication of refractory uranium compounds, summary report, Contract No. AT-(40-1)-2558. The Carborundum Company, Niagara Falls, New York.[12]

51. Tripler, A. B., M. J. Snyder, and W. H. Duckworth. 1959. A study of the effects of fabricating conditions on some properties of sintered uranium monocarbide. BMI-1383.[12]

52. Vordahl, M. B. 1962. Powder metallurgical processes and products. U. S. Patent 3,066,391.[13]

53. Watrous, J. D. 1960. Development of U-UC and uranium alloy-UC cermets. Trans. Am. Nuc. Soc. 3(1):131-132.

54. Weir, J. R. 1960. A failure analysis for the low temperature performance of dispersion fuel elements. Trans. Am. Nuc. Soc. 3(1):134.

55. Williams, J. 1960. Method of making uranium-uranium monocarbide cermet. U. S. Patent 2,965,480.[13]

---

[12]This report may be obtained from the Office of Technical Services, Department of Commerce, Washington 25, D. C.

[13]Copies of U. S. Patents may be obtained from the Department of Commerce, Patent Office, Washington 25, D. C.

APPENDIX A

Appendix Table 1. Specimen firing data

Sample No.	Batch No./gm	Initial Composition UC	UH_3	Other	(gm)	UC-U Ratio	Heat Press.	Firing Time	Firing Temp.	Pellet. Pressure	Pellet Density	Percent Theoret.
163-												
1a	C-1	14.70	6.38	.211 Acr[a]	--	70/30	Cold	--	210	19,650	--	--
1b	"	"	"	"	--	"	"	--	120	"	--	--
1	UH_3/5	--	5.00	.1 Acr	--	--	"	--	140	"	--	--
2	"	--	"	"	--	--	"	--	140	"	--	--
3	C-2/5	14.70	6.38	.1 Acr	--	70/30	"	--	109	"	--	--
4	"	--	"	"	--	"	"	--	95	"	--	--
5	UC/5	5.00	--	--	--	1	"	--	115	"	--	--
6	"	5.00	--	--	--	--	"	--	115	"	--	--
7		3.50	1.519	--	--	--	"	--	600	"	--	--
8	C-3	7.00	3.04	--	--	70/30	"	--	600	"	--	--
M-1	C-2/5	14.70	6.38	.1 Acr	--	"	"	--	120	"	--	--
M-2	UC/5	5.00	--	--	--	--	"	--	120	"	--	--
9	C-4/5	7.00	3.04	--	--	70/30	"	--	600	"	--	--
10	"	"	"	--	--	"	"	--	600	"	--	--
11	C-5/5	9.88	3.33	--	--	75/25	"	--	600	"	--	--
12a	C-7/5	7.00	2.26	--	--	"	"	--	1,150	"	--	--
12b	"	"	"	--	--	"	"	3	1,150	"	--	--
13	C-8/5	"	"	--	--	"	"	3	1,150	"	--	--
14	"	"	"	--	--	"	"	--	--	"	--	--
15	C-12/5	16.00	4.0664	--	.4StA[b]	80/20	"	--	600	"	--	--
16	"	"	"	--	"	"	"	3	1,500	"	--	--
17	C-10/6	"	"	--	--	"	"	--	--	"	--	--
18	C-11/5	16.00	4.0664	--	.4StA	"	"	1	1,500	2,000	--	--
19	UC/5	5.00	--	--	--	--	"	1	1,500	"	--	--
20	C-11/5	16.00	4.0664	--	.4StA	80/20	"	3	1,275	"	--	--

Continued

Appendix Table 1 (Continued)

Sample No.	Batch No./gm	Initial Composition UC	UH_3	Other	(gm)	UC-U Ratio	Heat Press.	Firing Time	Firing Temp.	Pellet. Pressure	Pellet Density	Percent Theoret.
21	C-21/5	16.00	4.0664	.1 Acr	.4StA	80/20	Cold	3	1,275	2,000	--	--
22	UH_3/5	--	5.00	--	--	--	"	--	--	"	--	--
23	C-13/5	16.00	4.0664	.4 Nap[c]	.4StA	80/20	"	1	1,000	"	--	--
24	"	"	"	"	"	"	"	1	1,000	40,000	--	--
25	C-18/5	17.00	2.962	.6 Nap	--	"	"	3	1,200	"	--	--
26	C-20/5	28.56	17.40	2.3 Nap	--	50/50	"	1	500	"	--	--
27	"	"	"	"	--	"	"	1	400	"	--	--
28	"	"	"	"	--	"	"	1	1,170	"	--	--
29	"	"	"	"	--	"	"	1	1,450	"	--	--
30	C-21/5	20.00	6.70	1.3 Nap	--	60/40	"	3	1,290	30,000	--	--
31	"	"	"	"	--	"	"	3	1,250	"	--	--
32	C-22/5	"	8.00	1.6 Nap	--	55/45	"	--	400	0	--	--
33	"	"	"	"	--	"	"	--	830	0	--	--
34	C-20/5	28.56	17.40	2.3	--	50/50	"	--	645	0	--	--
35	C-22/5	20.00	8.00	1.6	--	55/45	"	5	1,260	40,000	--	--
36	C-23/5	"	"	1.5	.84StA	"	Hot	1	1,150	2,000	--	--
37	C-21/5	"	6.70	1.3	--	60/40	"	1	1,160	"	--	--
38	C-20/5	28.56	17.40	2.3	--	50/50	"	1	1,260	"	--	--
39	C-23/5	20.00	8.00	1.5	.84StA	55/45	Cold	3	1,200	30,000	--	--
40	C-24/5	"	10.00	1.8	--	70/30	"	5	1,200	"	--	--
41	C-20/6	28.56	17.40	2.3	--	50/59	Hot	"	1,500	3,000	--	--
42	C-23/5	20.00	8.00	1.5	.84StA	55/45	Cold	"	1,160	40,000	--	--
43	C-24/6	"	10.00	1.8	--	70/30	"	"	1,160	"	--	--
44	C-20/7	28.56	17.40	2.3	--	50/50	Hot	1	1,175	4,000	--	--
45	C-23/6	20.00	8.00	1.5	.84StA	55/45	Cold	5	1,350	40,000	--	--
46	C-24/6	"	10.00	1.8	--	70/30	"	"	1,350	"	--	--
47	C-23/5	"	8.00	1.5	.84StA	55/45	"	--	--	"	--	--
48	C-26/6	40.00	21.54	1.5	2.0StA	65/35	"	10	1,200	"	--	--
49	C-24/6	20.00	10.00	1.8	--	70/30	"	"	"	"	--	--
50	C-26/5	40.00	21.54	1.5	2.0StA	65/35	Hot	5	1,175	4,000	--	--

Continued

Appendix Table 1 (Continued)

Sample No.	Batch No./gm	Initial Composition UC	UH_3	Other	(gm)	UC-U Ratio	Heat Press.	Firing Time	Firing Temp.	Pellet. Pressure	Pellet Density	Percent Theoret.
51	C-26/5	40.00	21.54	1.5	2.0StA	65/35	Hot	5	1,280	4,000	Poor	--
52	C-27/6	20.00	13.64	1.8	1.0StA	60/40	Cold	"	1,310	40,000	"	--
53	C-28/6	30.00	24.90	3.3	1.65StA	55/45	"	"	1,310	40,000	"	--
54	C-27/10	20.00	13.64	1.8	1.0StA	60/40	Hot	4	1,175	4,000	--	--
55	C-26/10	40.00	21.54	1.5	2.0StA	65/35	"	3	1,180	4,000	--	--
56	C-26/6	"	"		"	"	Cold	2	1,254	40,000	--	--
57	C-29/10	"	24.59	--	.718C	60/40	Hot	5	900	4,000	--	--
58	C-28/6	30.00	24.90	3.3	1.65StA	55/45	Cold	3	1,267	30,000	--	--
59	C-26/6	40.00	21.54	1.5	2.0StA	65/35	"	"	1,170	"	--	--
60	C-32/6	20.00	13.64	1.7	.34StA	60/40	"	"	1,200	"	--	--
61	C-28/6	30.00	24.90	3.3	1.65StA	55/45	"	"	1,200	"	--	--
62	C-30/6	20.00	13.64	1.7	.5StA	60/40	"	5	1,250	"	9.13	
63	C-33/5	20.00	13.64	1.7	.34StA	"	"	"	1,250	50 Tons	--	--
64	C-31/6	20.00	27.28	2.4	1.5StA	45/55	"	"	1,205	30,000	10.58	73.0
65	C-31/5	20.00	27.28	2.4	1.5StA	45/55	Hot	"	1,265	4,000		
66	C-30/6	20.00	13.64	1.7Nap	.5StA	60/40	Cold	1	1,350	30,000	--	--
67	C-31/6	20.00	27.28	2.4	1.5	45/55	"	"	1,370	"	10.61	--
68	C-32/6	20.00	13.64	1.7	.34	60/40	"	"	1,370	"	10.84	--
69	C-30/6	20.00	13.64	1.7	.5	60/40	"	"	1,441	"	10.63	--
70	C-31/6	20.00	27.28	2.4	1.5	45/55	"	"	1,470	"	10.48	--
71	C-32/6	20.00	13.64	1.7	.34	60/40	"	"	1,470	"	11.26	66.5
72	C-33/10	20.00	13.64	1.7	.34	60/40	Hot	3	1,200	3,000	--	--
73	C-31/6	20.00	27.28	2.4	1.5	75/55	Cold	--	--	30,000	--	--
74	C-32/6	20.00	13.64	1.7	.34	60/40	"	--	1,200	"	--	--
75	C-34/6	25.00	--	2.5	1.76	--	"	5	1,500	"	--	--
76	C-31/6	20.00	27.28	2.4	1.5	60/40	"	3	1,375	"	10.58	--
77	C-32/6	20.00	13.64	1.7	.34	60/40	"	"	1,375	"	--	--
78	C-39/6	25.00	--	2.5	1.76	--	"	1	1,530	"	--	--
79	C-35/10	20.00	13.64	2.0	--	60/40	Hot	3	1,212	3,000	--	--
80	C-44/10	10.00	6.82	--	--	60/40	"	"	1,200	"	12.2	--

Continued

Appendix Table 1 (Continued)

Sample No.	Batch No./gm	Initial Composition UC	UH_3	Other	(gm)	UC-U Ratio	Heat Press.	Firing Time	Firing Temp.	Pellet. Pressure	Pellet Density	Percent Theoret.
81	C-32/10	20.00	13.64	1.7	.34	60/40	Hot	1	1,276	1,540	9.4	78.5
82	C-43/8	25.00	16.95	--	--	60/40	"	2	1,300	3,000	--	--
83	C-43/10	25.00	16.95	--	--	60/40	"	1	980	3,000	10.68	77.7
84	C-46/8	10.00	6.82	--	--	60/40	"	20	1,550	3,000	12.2	97.5
85	C-45/10	10.00	6.82	--	--	60/40	"	1	1,104	3,000	10.4	83.9
86	/9.16	10.00	--	8.0 U	--	55/45	"	30	1,150	4,000	--	--
87	C-43/10	25.00	16.95	--	--	60/40	"	10	1,251	3,750	9.99	74.6
88	C-48/8	10.00	6.82	--	--	60/40	"	15	1,200	3,750	13.4	97.8
89	C-48/8	10.00	6.82	--	--	60/40	"	15	1,176	3,750	13.41	97.5
90	C-49/10	10.00	6.82	--	--	60/40	"	--		1,000	12.71	90.2
91	C-49/10	10.00	6.82	--	--	60/40	"	3	1,175	3,750	11.82	88.4
92	C-49/10	10.00	6.82	--	--	60/40	"	2	1,130	700	10.5	79.1
93	C-50/10	10.00	6.82	--	--	60/40	"	2	1,130	3,750	13.27	96.0
94	C-50/8	10.00	6.82	--	--	60/40	"	2	1,140	4,000	15.74	97.6
95	C-51/8	10.00	6.82	--	--	60/40	"	--	1,150	4,000	--	--
96	C-53/10	16.00	15.42	--	--	51/49	"	3	1,140	4,000	13.63	97.4
97	C-53/10	16.00	15.42	--	--	51/49	"	3	1,150	4,000	13.42	95.1
98	C-54/10	10.00	15.20	--	--	40/60	"	3	1,150	4,000	13.22	92.9
99	C-54/10	10.00	15.20	--	--	40/60	"	2	1,150	4,000	12.59	92.8
100	C-53/10	16.00	15.42	--	--	51/49	"	1	1,140	4,000	12.82	91.2

[a]Acr = Acryloid

[b]StA = Stearic Acid

[c]Nap = Naphthalene

APPENDIX B

Appendix Table 2. X-ray compositional analyses

Sample No.	Green X-ray Composition (%)				Fired X-ray Composition (%)			
	UC	UH_3	UO_2	Other	UC	U	UO_2	Other
163-30[a]	--	--	--	--	--	--	--	--
31	--	--	--	--	76.6	--	19.2	$4.2UC_2$
32	70.4	11.2	18.4	--	--	--	--	--
33	70.4	11.2	18.4	--	--	--	--	--
34	--	--	--	--	--	--	--	--
35	70.4	11.2	18.4	--	--	--	--	--
36	71.1	15.5	13.4	--	--	--	--	--
37	--	--	--	--	59.0	--	29.0	$12.0UC_2$
38	--	--	--	--	52.5	--	44.1	$3.4UC_2$
39	71.1	15.5	13.4	--	65.0	--	15.0	20.0 ?
40	--	--	--	--	80.0	--	10.0	10.0 ?
41	--	--	--	--	--	--	--	--
42	71.1	15.5	13.4	--	45.4	--	48.0	--
43	59.5	19.5	21.0	--	68.4	--	31.6	--
44	--	--	--	--	45.2	--	48.0	--
45	71.1	15.5	13.4	--	--	--	--	--
46	59.5	19.5	21.0	--	67.6	--	21.6	--
47	71.1	15.5	13.4	--	--	--	--	--
48	65.2	14.6	12.1	$8.1UC_2$	--	--	--	--
49	59.5	19.5	21.0	--	81.4	--	18.6	--
50	65.2	14.6	12.1	$8.1UC_2$	--	--	--	--
51	65.2	14.6	12.1	$8.1UC_2$	74.8	--	25.2	--
52	61.7	21.3	17.0	--	61.0	2.7	32.2	4.3?
53	55.4	23.2	21.4	--	61.5	9.9	29.4	--
54	61.7	21.3	17.0	--	59.0	--	41.0	--

Continued

Appendix Table 2 (Continued)

Sample No.	Green X-ray Composition (%)				Fired X-ray Composition (%)			
	UC	UH_3	UO_2	Other	UC	U	UO_2	Other
55	65.2	14.6	12.1	8.1UC	64.5	--	21.8	14.0 ?
56	65.2	14.6	12.1	8.1UC	--	--	--	--
57	--	27.6	72.4	--	--	--	--	--
58	55.4	23.2	21.4	--	--	--	--	--
59	65.2	14.6	12.1	8.1UC	--	--	--	--
60	57.3	12.7	26.2	3.8 ?	--	--	--	--
61	55.4	23.2	21.4	--	--	--	--	--
62	--	--	--	--	--	--	--	--
63	54.9	16.8	27.7	--	--	--	--	--
64	50.4	18.0	31.0	--	--	--	--	--
65	50.4	18.0	31.0	--	40.8	--	59.2	--
66	--	--	--	--	--	--	--	--
67	50.4	18.0	31.6	--	42.2	--	54.0	3.8 ?
68	57.3	12.7	26.2	3.8 ?	--	--	--	--
69	--	--	--	--	--	--	--	--
70	50.4	18.0	31.6	--	48.7	2.85	48.5	--
71	57.3	12.7	26.2	3.8 ?	66.5	2.81	30.7	--
72	54.9	16.8	25.7	--	--	--	--	--
73	50.4	18.0	31.6	--	--	--	--	--
74	57.3	12.7	26.2	3.8 ?	--	--	--	--
75	--	--	--	--	--	--	--	--
76	50.4	18.0	31.6	--	--	--	--	--
77	57.3	12.7	26.2	4.5 ?	--	--	--	--
78	--	--	--	--	--	--	--	--
79	54.2	13.3	28.0	--	10.9	--	70.2	19.0UC_2
80	56.0	38.0	9.0	--	52.3	--	47.7	
81	57.3	12.7	26.2	3.8 ?	61.2	--	38.8	
82	54.7	36.0	9.3		64.0	--	36.0	
83	54.7	36.0	9.3	--	63.0	15.0	19.0	
84	50.2	28.5	21.6	--	57.0	--	43.0	

Continued

Appendix Table 2 (Continued)

Sample No.	Green X-ray Composition (%)				Fired X-ray Composition (%)			
	UC	UH_3	UO_2	Other	UC	U	UO_2	Other
85	56.0	23.5	24.5	--	55.0	--	45.0	
86	--	--	--	--	82.0	Some	18.0	--
87	54.7	36.0	9.3	--	63.0	15.0	19.0	--
88	65.2	24.0	4.5	$6.3UC_2$	94.3	2.8	3.0	--
89	65.2	24.0	4.5	$6.3UC_2$	87.6	6.2	6.2	--
90	--	--	--	--	75.6	13.5	8.8	$2.1UC_2$
91	--	--	--	--	72.0	21.5	6.5	--
92	--	--	--	--	70.0	6.6	22.6	--
93	55.0	34.4	6.7	$3.9UC_2$	87.0	--	8.95	4.1 ?
94	--	--	--	--	81.6	11.9	6.5	--
95	52.4	40.0	3.8	$3.8UC_2$	--	--	--	--
96	50.4	41.2	4.2	$4.2UC_2$	83.7	10.3	6.0	--
97	50.4	41.2	4.2	$4.2UC_2$	76.3	14.0	9.8	--
98	50.5	38.5	5.5	$5.5UC_2$	58.5	28.5	11.5	--
99	50.5	38.5	5.5	$5.5UC_2$	59.1	28.2	12.8	--
100	51.2	39.5	4.0	$5.3UC_2$	58.2	20.5	18.0	$3.0UC_2$

[a]Specimens 1-29 not representative